

Universidade do Minho
Escola de Ciências

Humberto Henrique Gonçalves Pereira

**Metabolic engineering of acetyl-CoA
Carboxylase in *Saccharomyces cerevisiae***

Dissertação de Mestrado

Mestrado em Bioquímica Aplicada

Trabalho efetuado sob a orientação do

Professor Doutor Björn Johansson

Outubro de 2018

DECLARAÇÃO

Nome: Humberto Henrique Gonçalves Pereira

Endereço eletrónico: humbero14@gmail.pt **Telefone:** 912287268

Bilhete de Identidade/Cartão do Cidadão: 14191870

Título da dissertação: Metabolic engineering of acetyl-CoA carboxylase in *Saccharomyces cerevisiae*

Orientador: Professor Doutor Björn Johansson

Ano de conclusão: 2018

Designação do Mestrado: Mestrado em Bioquímica Aplicada, área de especialização em Biomedicina

É AUTORIZADA A REPRODUÇÃO INTEGRAL DESTA DISSERTAÇÃO APENAS PARA EFEITOS DE INVESTIGAÇÃO, MEDIANTE DECLARAÇÃO ESCRITA DO INTERESSADO, QUE A TAL SE COMPROMETE.

Universidade do Minho, 31/10/2018

Assinatura: _____

ACKNOWLEDGEMENTS

Agradeço calorosamente,

Aos meu orientador Björn Johansson pela disponibilidade, paciência e confiança que permitiram a produção do presente trabalho

Aos meus colegas de trabalho, Flávio, Paulo, Ricaro, Gabriel, Bia, Alexandra, Cláudia, Rosana, Pedro, Eduardo, Helena, Sofia e Mário pela entajuda laboratorial e por criarem um ambiente de trabalho agradável .

Aos técnicos do Departamento de Biologia, e em particular à Núria e ao sr. Luís pela assistência indispensável que prestaram.

À minha família, aos meus amigos e à Filipa pelo apoio e descontração que me recarregaram as energias para poder produzir este trabalho.

Muito obrigado!

Metabolic engineering of acetyl-CoA Carboxylase in *Saccharomyces cerevisiae*

ABSTRACT

Saccharomyces cerevisiae is one of the most studied microorganisms and one of the most used cell factories for the production of compounds with pharmacological value. The low intracellular concentration of Malonyl coenzyme A (malonyl-CoA) limits the ability of this yeast to produce malonyl-coA derived products such as flavonoids, polyketides and biodiesel. In this yeast, the only source of malonyl-CoA is the ATP-dependent carboxylation of acetyl coenzyme A (acetyl-CoA) catalyzed by acetyl-CoA carboxylase (ACC), the rate-limiting step in fatty acid biosynthesis. In this work, expression of heterologous ACCs in *S. cerevisiae* was attempted with the objective of establishing alternative malonyl-CoA production systems in this yeast. A *S. cerevisiae* strain with a tetracycline repressible *ACC1* was used for functional testing. Since *ACC1* is an essential gene, this strain is not capable of growing in medium supplemented with tetracycline. Expression of *S. cerevisiae* or *Yarrowia lipolytica* *ACC1* from a plasmid complemented the conditional phenotype and enabled growth in tetracycline containing medium. A plasmid expressing 4 genes coding for the *Arabidopsis thaliana* plastidic ACC subunits was unable to complement the phenotype. Expression of ACCs from plasmids caused prolonged lag phase, and specific growth rates were considerably lower than the ones obtained for the wild type strain. This result is consistent with previous studies where ACC activity was increased and likely results from the metabolic imbalance this increase might cause.

Engenharia metabólica de Acetyl-CoA Carboxilase em *Saccharomyces cerevisiae*

RESUMO

Saccharomyces cerevisiae é um dos microrganismos mais estudados e uma das fábricas celulares mais usadas na produção de compostos com valor farmacológico. A baixa concentração intracelular de malonil coenzima A limita a capacidade que esta levedura tem de produzir derivados deste metabolito, como flavonóides, policetídeos e biodiesel. Nesta levedura, a única fonte de malonil-coA é a carboxilação dependente de ATP de acetilcoenzima A realizada por acetyl-coA carboxylase (ACC), o passo limitante na biossíntese de ácidos gordos. Neste trabalho, foi tentada a expressão de ACCs heterólogos em *S. cerevisiae* com o objectivo de estabelecer sistemas alternativos de produção de malonil-coa nesta levedura. Uma estirpe de *S. cerevisiae* com um *ACC1* repressível foi usada para testes funcionais. Dado que *ACC1* se trata de um gene essencial, esta estirpe é incapaz de crescer num meio suplementado com tetraciclina. A expressão do *ACC1* tanto de *S. cerevisiae* como de *Yarrowia lipolytica* a partir de um plasmídeo complementou o fenótipo condicional e permitiu o crescimento num meio contendo tetraciclina. Um plasmídeo de expressão que codifica 4 genes codificantes para as subunidades da ACC plastídica de *Arabidopsis thaliana* foi incapaz de complementar o fenótipo. A expressão de *ACC1* a partir de plasmídeos causou uma fase de adaptação prolongada, e as taxas específicas de crescimento foram consideravelmente menores que as obtidas para a estirpe *wild type*. Este resultado é consistente com estudos anteriores onde a actividade de ACC foi aumentada e resulta, provavelmente, do desequilíbrio metabólico que este aumento pode causar.

TABLE OF CONTENTS

Acknowledgements.....	iii
Abstract.....	v
Resumo.....	vii
Table of contents.....	ix
List of figures.....	xi
List of tabels.....	xiii
List of abbreviations, initials and acronyms	xv
1. Introduction	1
1.1 Saccharamyces cerevisiae as cell factory	1
1.2 Significance of malonyl-coA in <i>Saccharomyces cerevisiae</i>	2
1.3 Increasing cellular pool of Malonyl-CoA	3
1.3.1 Acetyl-CoA carboxylase	4
1.3.2 Overexpression of ACC1 in <i>S. cerevisiae</i>	5
1.3.3 Heterologous ACCs expression in <i>S. cerevisiae</i>	6
1.4 Yeast Pathway Kit.....	8
1.5 Objectives	8
2. Materials and methods.....	11
2.1 Strains, Media and spectrophotometry.....	11
2.2 Genetics.....	13
2.2.1 Bioinformatics	13
2.2.2 Plasmid extraction	14
2.2.3 Yeast Chromosomal DNA extraction	14
2.2.4 Agarose gel electrophoresis	15
2.2.5 PCR conditions	15
2.2.6 Single gene expression cassettes construction.....	22
2.2.7 Activation of accD gene.....	24
2.2.8 Saccaromyces cervisiae transformation.....	25
2.2.9 Gel extraction of DNA.....	25
2.2.10 yEGFP fusion protein expression cassettes construction	26

2.2.11	Competent <i>E. coli</i> and transformation	26
2.2.12	MS-ACC gene cluster expression plasmids construction	27
2.2.13	Δ Acc Tet growth curves in tetracycline	28
2.3	Protein Biochemistry	29
2.3.1	Fluorescence microscopy.....	29
2.3.2	MCR extraction and SDS-PAGE.....	29
3.	Results and discussion.....	31
3.1	Confirmation of ACC Tet as a ACC activity testing strain	31
3.2	Heterologous expression of <i>Arabidopsis thaliana</i> MS-ACC in <i>S. cerevisiae</i>	33
3.2.1	Complete gene MS-ACC expression.....	33
3.2.2	yEGFP fusion proteins expression.....	36
3.2.3	Expression of genes without target peptide	40
3.2.4	Expression with activated accD	42
3.2.5	CAC2 gene and failure to complement conditional <i>ACC1</i> null mutation	45
3.3	Functional expression of <i>Y. lipolytica ACC1</i> in <i>S. cerevisiae</i>	46
3.3.1	Specific growth rate of clones expressin ScACC1 or YIACC1	48
3.4	MCR production	53
4.	Conclusion and future perspectives	55
5.	Bibliography.....	57
Anexo I – Designação do Anexo I		Error! Bookmark not defined.
Anexo II – Designação do Anexo II		Error! Bookmark not defined.

LIST OF FIGURES

Figure 1 - A , Native <i>S. cerevisiae</i> generation of malonyl-CoA from acetyl-coA, catalyzed by ACC. B , Malonyl-CoA production from malonic acid and coenzyme A, catalyzed by heterologous <i>Arabidopsis thaliana</i> malonyl-CoA synthetase (AAE13). Both reactions use ATP.	4
Figure 2 - Overall scheme of the partial reactions catalyzed by ACC.....	5
Figure 3 - Schematic representation of TP_Gene_TP assembly	24
Figure 4 - Growth rate formula.....	28
Figure 5 - Electrophoresis agarose gel of phusion polymerase PCR amplification of ScACC1	31
Figure 6 - Complementation of a conditional ACC1 null mutation by pYPK0_TEF1_ScACC1_TDH3 on solid YPD Tet medium.	32
Figure 7 - Electrophoresis agarose gel of PCR verification of the pYPK0_TEF1_ScACC1_TDH3 construct.....	32
Figure 8 - Electrophoresis agarose gel of PCR amplification of fragments CAC1, CAC2, CAC3 and accDin.....	33
Figure 9 - Electrophoresis agarose gel of colony PCR verification of MS-ACC unaltered single gene expression constructs	34
Figure 11 - Electrophoresis agarose gel of colony PCR verification of correct pYPK0_CAC1_CAC2_CAC3_accDin assembly.....	36
Figure 12 - Electrophoresis agarose gel of colony PCR screening of MS-ACC yEGFP fusion protein expression constructs	37
Figure 13 - Electrophoresis agarose gel of MS-ACC genes PCR amplification with addition of a linker coding sequence	38
Figure 15 - Electrophoresis agarose gel of MS-ACC amplifications without signal peptides.....	41
Figure 16 - Electrophoresis agarose gel of colony PCR screening of MS-ACC constructs without signal peptide.....	41
Figure 17 - SnapGene® software (from GSL Biotech; available at snapgene.com) DNA chronogram of sequenced accDin displaying the presence of a cytosine in the position 794.....	42
Figure 18 - Electrophoresis agarose gel of fragments accDF and accDT amplification at a T_A of 59 °C. A (847 bp), accDF amplification (primers 1057 and accD_C->T_rv). B (721 bp), accDT amplification (primers accD_C->T_fw and 973). M , molecular weight marker.....	43

Figure 19 - Electrophoresis agarose gel of colony PCR screening of pYPK0_FBA1_accDac_PDC1. Letters are colony PCRs using primers 577 and 1064 (1090 bp)	43
Figure 20 – Δ Acc Tet colonies containing a MS-ACC multiple gene cluster expression construct are unable to grow on solid YPD Tet medium	44
Figure 21 - Electrophoresis agarose gel of colony PCR screening of TEF1_CAC1-ps_TDH3_CAC2-ps_PGI1_CAC3-ps_FBA1_accDac_PDC1 and TEF1_CAC1-ps_TDH3_CAC2_PGI1_CAC3-ps_FBA1_accDac_PDC1	45
Figure 22 – ApE mediated comparison between theoretical CAC2 (upper sequence) and amplified CAC2 (bottom sequence).....	46
Figure 23 – Electrophoresis agarose gel of Phusion polymerase PCR amplification of both YIACC1 fragments at T_a of 60°C	47
Figure 24 - Complementation of a conditional ACC1 null mutation by pYPK0_TEF1_ScACC1_TDH3 on solid YPD Tet medium	47
Figure 25 - Electrophoresis agarose gel of colony PCR screening of pYPK0_TEF1_YIACC1_TDH3 construct.....	48
Figure 26 – Growth curves displaying the first 12h of growth in liquid YPD Tet. Each graphic plots the OD ₆₄₀ over time(h) for one of the 5 colonies measured	49
Figure 27 – a) Growth curves displaying the 12h or 24h (in the case of YIACC1) spans of time where the exponential growth phase was present for the strains that were capable of continuing growth in YPD Tet after the first 12h. b) Growth curves displaying the last 12h span of time for the strains that did not display additional growth after the first 12h.	50
Figure 28 – Comparison between growth rates (h^{-1}) of wild-type CEN.PK2-1C and Δ Acc Tet containing either pYPK0_TEF1_ScACC1_TDH3 construct (ScACC1) or pYPK0_TEF1_YIACC1_TDH3 construct (YIACC1).	51
Figure 28 - SDS-PAGE polyacrymide gel of MCR protein (132 kDa).	53

LIST OF TABLES

Table 1. Plasmids used in this work.....12

Table 2. Taq PCR solutions used in this work (without template).....16

Table 3. Primers used in this work.....16

Table 4. Template and primers used for confirmation PCR (usually colony PCR) in this work.....19

Table 5. Phusion PCR solutions used in this work (without template).....20

Table 6. Template and primers used for non-confirmation amplification in this work.....21

LIST OF ABBREVIATIONS, INITIALS AND ACRONYMS

3-HP	3-hydroxypropionic acid
<i>A. thaliana</i>	<i>Arabidopsis thaliana</i>
aa	amino acids
AAE13	plant malonyl-CoA synthetase gene of <i>Arabidopsis thaliana</i>
ACC	acetyl-coA carboxylase enzyme
<i>ACC1</i>	acetyl-coA carboxylase eukariotic gene 1
Acc1p	acetyl-coA carboxylase eukariotic gene 1 protein
<i>ACC1</i> ^{S1157A}	acetyl-coA carboxylase eukariotic gene 1, with Serine substituted by Adenine at residue 1157
<i>ACC1</i> ^{S659AS1157A}	acetyl-coA carboxylase eukariotic gene 1, with Serine substituted by Adenine at residue 1157
<i>ACC1</i> ^{S686AS659AS1157A}	acetyl-coA carboxylase eukariotic gene 1, with Serine substituted by Alanine at residue 1157
Ala	Alanine
APS	Ammonium Persulfate
ATP	adenosine triphosphate
BC	biotin carboxylase subunit
BCCP	biotin carboxyl carrier protein subunit
bp	base pair
cDNA	complementary DNA
CT- α	carboxyl transferase α
CT- β	carboxyl transferase β
DNA	Deoxyribonucleic acid
EMA	European Medicines Agency
FDA	Food and Drug Administration
FAEE	fatty acid ethyl esters
FAME	fatty acid methyl esters
GRAS	organism generally regarded as safe
h	hour
HFA1	<i>Sacharomyces cerevisiae</i> acetyl-coA carboxylase

Hfa1p	<i>Sacharomyces cerevisiae</i> acetyl-coA carboxylase protein
LB	Lysogeny Broth
MAE1	transmembrane dicarboxylic transporter from <i>Schizosaccharomyces pombe</i>
MCR	malonyl-CoA reductase
MF-ACC	Multifunctional acetyl-coa carboxylase enzyme
Min	minute
MS-ACC	Multi-subunit acetyl-coa carboxylase enzyme
OD	Optical Density
PAGE	Polyacrylamide Gel Electrophoresis
PKS	polyketide synthase
rcf	relative centrifugal force
rpm	revolutions per minute
s	second
<i>S. cerevisiae</i>	<i>Saccharomyces cerevisiae</i>
SAP	Shrimp Alkaline Phosphatase
<i>ScACC1</i>	<i>ACC1</i> gene of <i>Saccharomyces cerevisiae</i>
SD	Synthetic Defined medium
SDS	Sodium Dodecyl Sulphate
SDS-PAGE	Polyacrylamide Gel Electrophoresis
Ser1157	Serine residue at position 1157
Ser659	Serine residue at position 659
Ser686	Serine residue at position 685
TE	1 mL TrisHCl (pH 7.4) 50 mM, EDTA 1 mM
TEMED	N,N,N',N'-Tetramethylethylenediamine
TP	terminator-promoter
ws2	<i>hydrocarbonoclasticus</i> wax ester synthase gene
<i>Y. lipolytica</i>	<i>Yarrowia lipolytica</i>
<i>YIACC1</i>	<i>ACC1</i> gene of <i>Yarrowia lipolytica</i>
YNB w/o aa	Yeast Nitrogen Base without aminoacids
YPD	Yeast extract Peptone Dextrose
YPD tet	YPD medium supplemented with 111 mg/L tetracycline

YPK

Yeast Pathway Kit

1. INTRODUCTION

1.1 *Saccharomyces cerevisiae* as cell factory

The traditional importance of *Saccharomyces cerevisiae* (*S. cerevisiae*) in wine, beer and bread production led to research being historically focused on it (Barnett, 2003). This yeast is, today, one of the most well understood microorganisms, whose body of knowledge includes the complete sequencing of *S. cerevisiae* genome (Goffeau et al., 1996) and the *Saccharomyces* Genome Deletion Project (Winzeler et al., 1999). A wealth of genetic engineering tools is also available for use in this yeast. These include expression vectors (Böer et al., 2007), genetic selection markers (Siewers, 2014), reporter genes (Haar et al., 2007), and highly efficient transformation methods (Gietz & Schiestl, 2008; Yoshiyuki et al., 2002). *S. cerevisiae* has also a high efficiency of homologous recombination that allows targeted manipulations within its genome (Klinner & Schäfer, 2004).

S. cerevisiae is an attractive microorganism to use in an industrial setting. Its resistance to acidic environments (X. Liu et al., 2015) as well as high concentrations of sugar (Narendranath & Power, 2005) and ethanol (Hu et al., 2007) lowers the risk of contamination in industrial fermentation (Beckner et al., 2011). Furthermore, this yeast is fairly tolerant to inhibitors present in biomass hydrolysates (Jönsson et al., 2013). The fact that *S. cerevisiae* is able to grow anaerobically can reduce the need for oxygenation of the media, depending on the desired product (Ishtar Snoek & Yde Steensma, 2007). This yeast's capacity of producing high amounts of ethanol attests this yeast's capability of converting a carbon source into a metabolite of economic value (Mohd Azhar et al., 2017). Production of compounds via *S. cerevisiae* biosynthesis can be sustainable and independent of oil supply as it depends on renewable raw material such as glucose or fructose derived from starch or sucrose (Borodina & Nielsen, 2014). Pentoses derived from lignocellulose are also a promising material to be used by recombinant *S. cerevisiae* capable of utilizing these carbon sources (Costa et al., 2017; Kötter et al., 1990). This is especially relevant when one considers that lignocellulosic materials include low-cost residues from agriculture, forestry and industry as well as dedicated lignocellulosic crops. Pentoses can represent more than 20% of dry material by weight in this materials (Cherubini, 2010). Adding to this the fact that *S. cerevisiae* is considered a "generally regarded as safe" (GRAS) organism by the Food and Drug Administration (FDA), it becomes apparent why roughly 13% of biopharmaceutical products approved by this agency and the European Medicines Agency (EMA)

between 2003 and 2013 were produced using this yeast (Baeshen et al., 2014). Health related substances produced by *S. cerevisiae* include insulin precursors (Kjeldsen, 2000), anti-malarial drug precursors (Paddon et al., 2013; Westfall et al., 2012), and human papilloma virus and hepatitis B vaccines (McAleer et al., 1984; Schillera et al., 2008).

1.2 Significance of malonyl-coA in *Saccharomyces cerevisiae*

Malonyl-CoA is an important precursor for a range of pharmacologically relevant products, including flavonoids, stilbenoids and polyketides (H. Chen et al., 2011; Choi & Da Silva, 2014). Flavonoids and stilbenoids are phenolic compounds with promising applications as antimicrobial (Araya-Cloutier et al., 2017; Seleem et al., 2017), anticancer (Batra & Sharma, 2013), and anti-inflammatory agents (González et al., 2011). On the other hand, the pharmacological usefulness of polyketides is already established in the form of the cholesterol-lowering statins, tetracycline antibiotics, and doxorubicin anticancer agents (Crawford & Townsend, 2010). The first successful heterologous production of stilbenoids with no need for feeding of expensive precursors was performed in *S. cerevisiae* (M. Li et al., 2016). *De novo* biosynthesis of flavonoids (Rodriguez et al., 2017) and polyketides (Wattanachaisaereekul et al., 2007) has also been achieved in this yeast. *S. cerevisiae* is of particular interest when it comes to polyketide production for two main reasons: this yeast is thought to have a similar codon usage to the polyketide producing filamentous fungi due to taxonomical proximity; the high efficiency of homologous recombination in this yeast allows for accurate manipulation of large DNA fragments such as polyketide synthase (PKS) genes. In fact, heterologous expression of putative genes in *S. cerevisiae* has been successfully used for the functional screening of new PKSs (Tsunematsu et al., 2013).

Malonyl-CoA derived products also include non-pharmacological substances with economic value such as fatty alcohols, 3-hydroxypropionic acid (3-HP) and biodiesel. In *S. cerevisiae* production of all three has been shown to be raised by increasing intracellular malonyl-CoA supply (Feng et al., 2015; Shi et al., 2014). Fatty alcohols are long-chain alcohols that are currently used in the manufacturing of emulsifiers, cosmetics, lubricants and detergents (Feng et al., 2015; G. Wang et al., 2016; Zheng et al., 2012). And 3-HP can be used to produce numerous valuable chemicals and polymers such as acrylic acid, acrylamide, acrylonitrile, 1,3-propanediol, and malonic acid (Y. Chen & Nielsen, 2013). Biodiesel, on the other hand, is a greener alternative to fossil fuels that can be used in normal unmodified diesel engines (Hasan & Rahman, 2017; Selvaraj et al., 2016). However, the high

production costs due to the prices of oil feedstock (more than 75% of the production cost), labour and catalyst make it more expensive than conventional diesel, preventing it from being economically feasible (Atabani et al., 2012; Hasan & Rahman, 2017). It is, therefore, important to find alternative ways to generate biodiesel. The most common methods of biodiesel production involve catalysed transesterification of vegetable oil and alcohol (usually methanol or ethanol) to yield glycerol and fatty acid alkyl esters (usually fatty acid methyl esters (FAME) or fatty acid ethyl esters (FAEE))(Gashaw et al., 2015; Kumar et al., 2013). Using yeast for biodiesel production could negate catalyst expenses by bypass this transesterification step: The heterologous expression of the *Marinobacter hydrocarbonoclasticus* wax ester synthase gene *ws2* to synthesize FAEE directly from ethanol and acyl coenzyme A is something that has been demonstrated in *S. cerevisiae* (Shi et al., 2012; Valle-Rodríguez et al., 2014). Furthermore the use of this yeast could widen the type of biodiesel producing feedstocks to include the cheaper materials already used in bioethanol production, as well as the previously mentioned prospective low-cost lignocellulosic biomass (Sheng & Feng, 2015).

1.3 Increasing cellular pool of Malonyl-CoA

S. cerevisiae relies mainly on acetyl coenzyme A carboxylase (ACC) to produce malonyl-CoA through the adenosine triphosphate (ATP) dependent carboxylation of acetyl-CoA (Fig.1)(Tehlivets et al., 2007). However, this enzyme is under tight transcriptional and posttranslational regulatory control (Xiaoxu Chen et al., 2017; Hofbauer et al., 2014; Lian & Zhao, 2014), and this yeast maintains a very limited cellular pool of malonyl-CoA (Y. Wang et al., 2014).Furthermore, *S. cerevisiae* accumulates storage lipids in low amounts and is considered a nonoleginous yeast (Fakas, 2017; Knoshaug et al., 2018). In fact, neither storage lipids nor lipid bodies seem to be essential for growth in this yeast (Sandager et al., 2002). It is, therefore, important to find ways to increase intracellular malonyl-CoA, if *S. cerevisiae* is to become an effective cell factory for malonyl-coA derived products. One approach that has proved effective at this involved the inhibition of fatty acid biosynthesis (Xiaoxu Chen et al., 2017). However, this is not relevant if the products to be generated are fatty acid derivatives. The heterologous expression of *Arabidopsis thaliana* (*A. thaliana*) malonyl-CoA synthetase (AAE13) capable of generating malonyl-CoA from malonic acid and coenzyme A has been shown to increase accumulation of both endogenous triacylglycerol and heterologous reverestrol (simultaneously stilbenoid and polyketide) to 1.6 and 2.4 fold respectively in this yeast (Y. Wang et al., 2014). However, the low intracellular concentration of malonic acid in *S. cerevisiae* means that malonic acid supplementation is required for

this strategy to be further improved. Since this yeast lacks the ability to uptake exogenous malonic, the heterologous expression of a transmembrane dicarboxylic transporter (MAE1) from *Schizosaccharomyces pombe* was needed in order to endow *S. cerevisiae* with this ability (W. N. Chen & Tan, 2013). Improving acetyl-coA supply has also proved effective at increasing the generation of malonyl-coA derived products (W. Liu et al., 2017; Seip et al., 2013). Nonetheless, when it comes to increasing malonyl-coA production, the approaches that have received the most attention involve enhancing ACC activity (Lian & Zhao, 2014; Y. Wang et al., 2014).

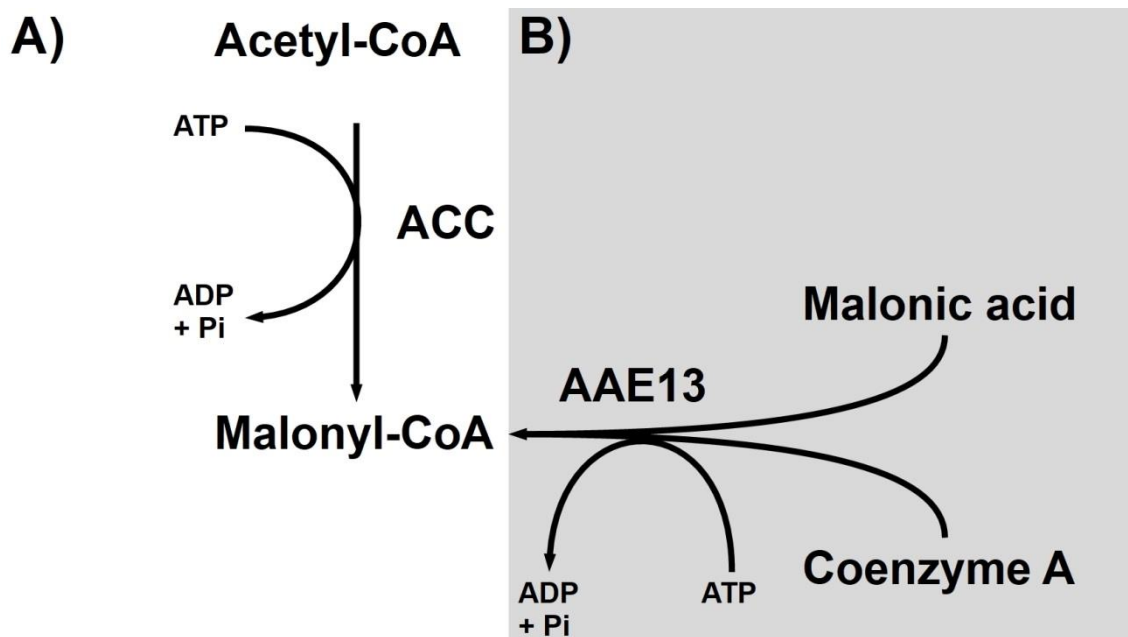


Figure 1 - A, Native *S. cerevisiae* generation of malonyl-CoA from acetyl-coA, catalyzed by ACC. **B**, Malonyl-CoA production from malonic acid and coenzyme A, catalyzed by heterologous *Arabidopsis thaliana* malonyl-CoA synthetase (AAE13). Both reactions use ATP.

1.3.1 Acetyl-CoA carboxylase

The carboxylation of acetyl-CoA to malonyl-CoA by ACC is both the committed and the rate limiting step in lipid biosynthesis (Hunkeler et al., 2016). There are two main types of ACC: multi-subunit ACC (MS-ACC) and multifunctional ACC (MF-ACC). MS-ACC is present in bacteria and in most plant plastids and is a heteromeric enzyme made up of 4 different kinds of monomers: biotin carboxylase (BC), biotin carboxyl carrier protein (BCCP), and carboxyl transferase α and β (CT- α and CT- β) (Salie & Thelen, 2016; Tong & Harwood, 2006). MF-ACC, on the other hand, is a homomeric enzyme found in the cytosol of eukaryotes and combines all functional components into a single ~ 250 kDa polypeptide chain (Yukiko Sasaki & Nagano, 2004). A whole third of the MF-ACC consists of the central region whose function is still poorly characterized. It probably acts as a scaffold to position BC

and CT correctly for catalyses. It also regulates ACC activity via phosphorylation of at least one serine residue. This region is not found in MS-ACC (Hunkeler et al., 2016; Wei et al., 2016). The reaction catalysed by both types of ACC is the same: first, BC catalyses the attachment of a carboxyl group from bicarbonate to biotin in an ATP dependent reaction; then, biotin carries this carboxyl group to the active site of CT where it is transferred to acetyl-CoA to form malonyl-coA (Fig. 2)(Cronan & Waldrop, 2002).

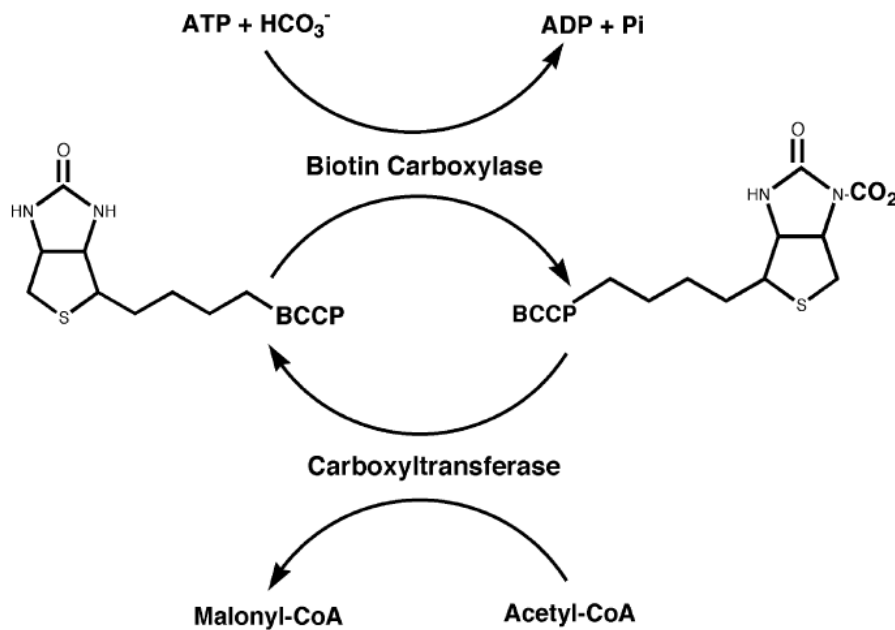


Figure 2 - Overall scheme of the partial reactions catalyzed by ACC. ATP spending allows the formation of biotin carboxyl. Biotin carboxyl then transports the carboxyl group to CT where it reacts with acetyl-CoA to form malonyl-CoA adapted from Cronan & Waldrop, 2002.

1.3.2 Overexpression of ACC1 in *S. cerevisiae*

S. cerevisiae chromosomal genome encodes two multifunctional ACCs: one cytosolic (*ACC1* - YNR016C) and one mitochondrial (*HFA1*). Hfa1p has the role of providing intraorganellar malonyl-coA which is required for the production of lipoic acid, a cofactor essential for aerobic metabolism (Hoja et al., 2004). Nonetheless, since the majority of biosynthetic processes happens in the cytosol, attempts at increasing *S. cerevisiae* ACC activity overwhelmingly focus in *ACC1* (Lian & Zhao, 2014). The overexpression of *ACC1* alone has been successfully used for the increased production of silbenoids (S. Y. Shin et al., 2012), polyketides (S. Y. Shin et al., 2012; Wattanachaisaareekul et al., 2008), fatty alcohols (Feng et al., 2015), 3-HP (Y. Chen et al., 2014; Shi et al., 2014), biodiesel (Shi et al., 2014), and fatty acids (Runguphan & Keasling, 2014; Shi et al., 2014; G. H. Shin et al., 2012; J. Wang et al., 2016). However, with the exception of G. H. Shin et al., 2012, none of these cases led to an increased

production of more than 2 fold. Furthermore, there is at least one instance where *ACC1* overexpression was unsuccessful at increasing fatty acid generation (Xiaowei Li et al., 2014). These cases highlight the strong posttranslational control this enzyme is under. Acc1p activity is negatively regulated via phosphorylation mediated by AMP-activated protein kinase Snf1p (Wei et al., 2016). However, *Snf1* deletion with or without *ACC1* overexpression failed to increase fatty alcohol production. This is probably due to *Snf1* being a regulatory gene with other targets apart from *ACC1*, which can negate the positive effects of *ACC1* deregulation (Feng et al., 2015). Three serine residues are known to be targeted by Snf1p in *S. cerevisiae*: Ser659, Ser686 and Ser1157. Site-directed mutagenesis has been effective at abolishing this kind of regulation. Through alignment of both sequences, it was possible to match *S. cerevisiae* Acc1p Ser1157 with Ser1215 of *Rattus norvegicus* Acc1p, a serine residue that had previously been reported as a target of AMP-activated protein kinase (AMPK), the mammalian ortholog of Snf1p. Overexpression of a *S. cerevisiae* *ACC1* mutated to Ala at Ser1157 (*ACC1*^{S1157A}) resulted in increased ACC activity, as well as increased polyketide and fatty acid yield, when compared with overexpression of the unmutated gene (Choi & Da Silva, 2014; M. Zhang et al., 2013). Ser659 was identified by searching for the phosphorylation recognition motif (Hyd-X-Arg-XX-Ser-XXX-Hyd) for Snf1. A Ser1157 and Ser659 to Ala *ACC1* mutant (*ACC1*^{S659AS1157A}) was shown to further increase ACC activity in comparison to *ACC1*^{S1157A}, when overexpressed. This resulted in even higher generation of 3-HP and biodiesel (Shi et al., 2014) than *ACC1*^{S1157A}. More recently, 13 mutations in previously described phosphorylated sites were screened for malonyl-coA production by use of a malonyl-coA sensor. This led to the creation of an *ACC1* mutated to Ala at Ser1157, Ser659 and Ser686 (*ACC1*^{S686AS659AS1157A}) that was able to further improve intracellular malonyl-coa levels, as well as 3-HP yield when compared with *ACC1*^{S659AS1157A} (Xiaoxu Chen et al., 2018).

1.3.3 Heterologous ACCs expression in *S. cerevisiae*

Plants usually possess both MF-ACC and MS-ACC. MF-ACC is present in the cytosol and is responsible for the synthesis of cytosolic malonyl-CoA which is used in a number of pathways, including polyketide and flavonoids biosynthesis, elongation of very-long-chain fatty acids, and malonylation of D-amino acids (Yukiko Sasaki & Nagano, 2004). MS-ACC, on the other hand, is present in the plastids and is responsible for the production of plastidic malonyl-CoA which is used for the *de novo* synthesis of fatty acids. In plants, each of the MS-ACC subunits is coded by a different gene. In modern plants, BC, BCCP and CT- α are coded in the nucleus and CT- β coded in the plastids, while in some primitive plants only BC is coded in the chromosome (Cronan & Waldrop, 2002). Plant MS-ACC is regulated in a

distinct manner to *S. cerevisiae ACC1* and is capable of generating high lipid concentration in seeds (Li-Beisson et al., 2013; Moser, 2010; Salie & Thelen, 2016). This may hint to the possibility of this enzyme increasing ACC activity if heterologously expressed in yeast. There is at least one example of *S. cerevisiae* heterologously expressing a plant ACC. And this is in the form of a wheat MF-ACC, with no insights of effect in lipid production (Joachimiak et al., 1997). This is also true for the heterologous expression of a bacterial MS-ACC from *Corynebacterium glutamicum* in this yeast, which improved fatty acid production by 1.6 fold (You et al., 2017). As for other yeasts, Wan et al., 2004 were capable of endowing *Pichia pastoris* with resistance to soraphen A, a potent inhibitor of fungal ACC, via expression of *Escherichia coli* MS-ACC. The authors gave the name of sor^R to a construct containing all four MS-ACC genes and patented this selection marker (US008088623B2, 2012).

Oleaginous yeasts are defined as yeasts capable of storing lipids in amounts greater than 20% of dry weight (Meng et al., 2009). In these yeasts, the main source of acetyl-CoA comes from the cleavage of citrate to oxaloacetate and acetyl-coA by use of coenzyme A in an ATP dependent reaction catalysed by ATP:citrate lyase (Ratlidge, 2002). This contrasts with nonoleaginous yeasts where acetyl-coA is exclusively generated by acetyl-CoA synthetase from acetate and Coenzyme A in an ATP dependent reaction (Galdieri et al., 2014). Under nitrogen limiting conditions, intracellular levels of citrate increase. This larger pool of citrate upregulates ATP:citrate lyase mediated production of acetyl-CoA (Fakas, 2017). Oleaginous yeasts, thus, accumulate more lipids when grown in nitrogen limiting conditions. This happens when the ratio between total mass of carbon and nitrogen (C/N) in the medium is greater than 20 (Papanikolaou & Aggelis, 2011). However ATP:citrate lyase activity seems not to be the sole determining factor in lipid accumulation, since it is also present in some nonoleaginous species (Adams et al., 2002). Furthermore, the fact that oleaginous yeasts are capable of taking advantage of this increased pool of acetyl-coA could suggest ACC activity as one of the contributing factors. Overexpression of native *ACC1* in oleaginous *Rhodospiridium toruloides* and *Yarrowia lipolytica* (*Y. lipolytica*) has been successfully used to increase lipid accumulation in these yeasts (Qiao et al., 2015; Tai & Stephanopoulos, 2013; S. Zhang et al., 2016). Heterologous expression of *ACC1* from oleaginous fungus *Mucor rouxii* in nonoleaginous yeast *Hansenula polymorpha* was successful at increasing total fatty acid content (Ruenwai et al., 2009). In *S. cerevisiae*, heterologous expression of *ACC1* from *Lipomyces starkeyi* was capable of enhancing lipid accumulation, although not more than overexpression of the native *ACC1*. The authors suggest codon usage differences between the two yeasts might be to blame for this lack of difference (J. Wang et al., 2016).

1.4 Yeast Pathway Kit

Metabolic engineering might require the introduction of multiple genes in order to change a particular trait. This is the case when trying to express a multi-subunit enzyme (You et al., 2017) or multiple enzymes involved in a metabolic pathway (W. Liu et al., 2017). The utilization of traditional means of genetic engineering like the one gene per plasmid approach makes this a laborious and problematic endeavour due to issues such as plasmid incompatibility as well as the limited number of selection markers that can be used (Novick, 1987). This led to the creation of approaches that allow simultaneous assembly of multiple DNA fragments, such as the *in-vitro* enzymatic assembly called “DNA assembler” (Shao et al., 2009) or the Gibson assembly method which relies on *in-vivo* homologous recombination of DNA fragments (Gibson, 2009).

Yeast Pathway Kit (YPK) was the approach that was chosen in this work. In this method the genes, promoters and terminators are cloned in one of three closely spaced blunt restriction sites in the pYPKa plasmid. The short stretches of plasmid backbone sequences between the three cloning sites provide homologous sequences for assembly of promoter-gene-terminator expression cassettes. The promoters and terminators used are designated terminator-promoters (TPs) as they are intergenic sequences from genes expressed in tandem in *S. cerevisiae* and function both as terminators for the upstream gene and promoters for the downstream gene. An expression cassette with a specific TP as terminator can be joined to one that has the same TP as a promoter by homologous recombination. This can, in turn, be used to generate a multiple gene expression construct (Pereira et al., 2016).

1.5 Objectives

The main goal of this work was the improvement of intracellular malonyl-coA levels in *S. cerevisiae* through the functional expression of heterologous ACCs. Two distinct types of ACC were chosen, the plastidic MS-ACC of *A. thaliana* and the MF-ACC of *Y. lipolytica*. The choice of *A. thaliana* ACC was grounded on the status of this organism as an extensively studied plant model (Koorneef & Meinke, 2010) and in complementary DNA (cDNA) availability. Similarly, *Y. lipolytica* was chosen due to being one of the most well studied oleaginous yeasts (Fakas, 2017; Mirończuk et al., 2016). Furthermore this yeast belongs to same phylogenetic family as *S. cerevisiae*, Saccharomycetaceae (Mühlhausen & Kollmar, 2014). This means that cDNA might not be required, since alternative splicing is likely to be similar in *S. cerevisiae*. YPK was used in order to express these heterologous ACCs in *S. cerevisiae*. Functional expression was verified through their ability to complement a conditional *ACC1*

null mutation in this yeast. A multitude of molecular biology approaches were used so as to tackle the lack of functional expression in certain constructs.

2. MATERIALS AND METHODS

2.1 Strains, Media and spectrophotometry

All plasmids used in this study are listed in table 1. These were propagated in *Escherichia coli* (*E. coli*) XL1-Blue (Stratagene) and selected on 2% (w/v) agar LB medium (0.5% (w/v) Bacto™ yeast extract, 1% (w/v) Bacto™ tryptone, 1% (w/v) NaCl) supplemented with 100 mg/L ampicillin (LB Amp) at 37°C. *Saccharomyces cerevisiae* strains CEN.PK113-5D (MATa ura3-52 HIS3, LEU2 TRP1 MAL2-8c SUC2) and Δ Acc Tet were used in this work. Δ Acc Tet is a CEN.PK2-1C (MATa ura3-52 his3- Δ 1 leu2-3,112 trp1-289, MAL2-8c SUC2) that has had its *ACC1* promoter substituted with the loxP-KanMX4-loxP-TDH3p-tc-3xHA cassette described in Kötter et al., 2009. This alteration prevents the essential *ACC1* gene (Tehlivets et al., 2007) from being expressed in the presence of Tetracycline. CEN.PK 113-5D was used for cassette construction of each single subunit of MS-ACC. Δ Acc Tet was used for the creations of both MF-ACC and MS-ACC constructs. Yeast strains were maintained at 30°C on 2% (w/v) agar YPD medium (1% (w/v) Bacto™ yeast extract, 1% (w/v) Bacto™ peptone, 2% (w/v) glucose), defined medium (6.7 g/L Difco YNB w/o aa, 2% (w/v) glucose) or SD URA- medium (Ramsdale dropout amino acid mixture w/o Ura - Appendix I). 2% (w/v) agar YPD medium supplemented with 111 mg/L tetracycline (YPD Tet) was used to select constructs in Δ Acc Tet that resulted in functional ACC. The liquid versions of the above-mentioned media were used as required for different applications throughout this work. Apart from growth curves, every growth in liquid medium was performed at 200 rpm. When growing a culture starting from a specific optical density (OD) the cells are first inoculated into a starter culture and incubated overnight. The OD of this starter culture is then determined by measuring a sample at 1:10 (culture:medium) dilution so as to keep the OD within the linear range. This data is used to calculate the volume of starter culture that will be used to initiate a culture at the specific chosen OD in the volume of medium to be used. Spectrophotometry was performed at a wavelength of 640 nm (OD₆₄₀) for yeast and 600 nm (OD₆₀₀) or 578 nm (OD₅₇₈) for bacteria in a GENESYS™ 20 Visible Spectrophotometer. Sterile growth medium was used as control.

Table 1. Plasmids used in this work.

Plasmids	Description	Reference
pYPKpw	Shuttle vector used for pathway constructions; Amp ^r ; URA3	(Pereira et al., 2016)
pYPKa_Z_TEF1	Plasmids with TPs cloned in the <i>ZraI</i> restriction site; Amp ^r	(Pereira et al., 2016)
pYPKa_Z_TDH3		
pYPKa_Z_PGI1		
pYPKa_Z_FBA1		
pYPKa_Z_RPL5		
pYPKa_E_TDH3	Plasmids with TPs cloned in the <i>EcoRV</i> restriction site; Amp ^r	(Pereira et al., 2016)
pYPKa_E_PGI1		
pYPKa_E_FBA1		
pYPKa_E_PDC1		
pYPKa_E_RPL5		
pYPK0_TEF1_ScACC1_TDH3		
pYPK0_TEF1_YIACC1_TDH3	pYPKpw derivative expressing <i>YIACC1</i>	This work
pYPK0_TEF1_CAC1_TDH3	pYPKpw derivative expressing CAC1	This work
pYPK0_TDH3_CAC2_PGI1	pYPKpw derivative expressing CAC2	This work
pYPK0_PGI1_CAC3_FBA1	pYPKpw derivative expressing CAC3	This work
pYPK0_FBA1_accDin_PDC1	pYPKpw derivative expressing <i>accDin</i>	This work
pYPK0_FBA1_accDac_PDC1	pYPKpw derivative expressing <i>accDac</i>	This work
pYPK0_TDH3_CAC2_RPL5	pYPKpw derivative expressing CAC2	This work
pYPK0_RPL5_CAC3_FBA1	pYPKpw derivative expressing CAC3	This work
pYPK0_TEF1_CAC1-ps_TDH3	pYPKpw derivative expressing CAC1-ps	This work
pYPK0_TDH3_CAC2-ps_PGI1	pYPKpw derivative expressing CAC2-ps	This work
pYPK0_PGI1_CAC3-ps_FBA1	pYPKpw derivative expressing CAC3-ps	This work
pYPK0_TEF1_CAC1-yEGFP_TDH3	pYPKpw derivative expressing CAC1-yEGFP	This work
pYPK0_TDH3_CAC2-yEGFP_PGI1	pYPKpw derivative expressing CAC2-yEGFP	This work
pYPK0_PGI1_CAC3-yEGFP_FBA1	pYPKpw derivative expressing CAC3-yEGFP	This work

pYPK0_FBA1_accDin-yEGFP_PDC1	pYPKpw derivative expressing <i>accDin</i> -yEGFP_PDC1	This work
pYPK0_CAC1_CAC2_CAC3_accDin_(PGI1 -> RPL5)	pYPKpw derivative expressing CAC1, CAC2, CAC3 and <i>accDin</i>	This work
pYPK0_CAC1-ps_CAC2-ps_CAC3-ps_accDin	pYPKpw derivative expressing CAC1-ps, CAC2-ps, CAC3-ps and <i>accDin</i>	This work
pYPK0_CAC1_CAC2_CAC3_accDac	pYPKpw derivative expressing CAC1, CAC2, CAC3 and <i>accDin</i>	This work
pYPK0_CAC1-ps_CAC2-ps_CAC3-ps_accDac	pYPKpw derivative expressing CAC1-ps, CAC2-ps, CAC3-ps and <i>accDac</i>	This work
pYPK0_CAC1-ps_CAC2_CAC3-ps_accDac	pYPKpw derivative expressing CAC1-ps, CAC2, CAC3-ps, <i>accDac</i>	This work
pYPK0_CAC1_CAC2_CAC3_accDin	pYPKpw derivative expressing CAC1, CAC2, CAC3 and <i>accDin</i>	This work
pTrc_Mcr-Ca	Plasmid used for <i>E. coli</i> expression of MCR; Amp ^r	(Kroeger et al., 2011)

2.2 Genetics

2.2.1 Bioinformatics

Gene sequences were obtained from GenBank database (Benson et al., 2005). Signal peptide sequences for each gene were obtained from UniProt database (Wu et al., 2006). TP1_Gene_TP2 (Table 1, 12th to 20th rows) and pYPK0_CAC1_CAC2_CAC3_accDin constructs, as well as respective primers sequences were created via ypkpathway (Pereira et al., 2016). The remaining constructs (Table 1, 21st to 33rd rows) and respective primers sequences were based on the previous sequences and were designed using *SnapGene*® software (from GSL Biotech; available at snapgene.com). This tool and ApE - A Plasmid Editor (Davis, 2016) were both used for determination of homology between sequences and for DNA chromatogram visualization of sequenced DNA. Sanger sequencing by GATC Biotech (Konstanz, Germany) was the sequencing used in this work. “WebPCR” online tool (Johansson, <http://www.webpcr.appspot.com/>) was used to determine ideal annealing temperatures (T_A) for primer pairs. Thermofischer online tool “Multiple Primer Analyzer” was used in order to determine possible

primer dimer formation (Thermofisher, <https://www.thermofisher.com/pt/en/home/brands/thermo-scientific/molecular-biology/molecular-biology-learning-center/molecular-biology-resource-library/thermo-scientific-web-tools/multiple-primer-analyzer.html>). ApE - A Plasmid Editor (Davis, 2016) was also used to confirm sequenced TP1_Gene_TP2 constructs. The online National Center for Biotechnology Information Basic local alignment search tool (NCBI BLAST) was used when pertinent (Johnson et al., 2008).

2.2.2 Plasmid extraction

A single colony of cells with the desired plasmid was used to initiate a 10 mL liquid culture the day before extraction. *E. coli* cultures were grown in LB Amp and yeast cultures were grown either in YPD or SD URA-. Extractions were achieved by using protocol A of *GeneJET Plasmid Miniprep Kit (Thermo Scientific™)*. When extracting plasmids from yeast this protocol was also used, but two addendums were added between step 1 and 2 of the protocol: 15 U of zymolyase were added to the resuspended cells and an enzymatic lysis was performed at 37°C during 3h; Following this step, mechanic lysis was performed by use of glass beads for 3 min. Success of an extraction was determined by PCR followed by agarose gel electrophoresis. DNA meant for sequencing was also quantified by spectrometry using *NanoDrop® ND-1000 Spectrophotometer* so as to ensure concentration requirements were met.

2.2.3 Yeast Chromosomal DNA extraction

The same genomic DNA extraction method was used for both *S. cerevisiae* and *Y. lipolytica*. The only difference is that the *S. cerevisiae* CEN.PK102-3A cell culture was grown overnight in 15 mL YPD while the *Y. lipolytica* PYCC 3347 cell culture was grown over 4 days in 50 mL . The culture was centrifuged for 5 min at 4500 rcf and the supernatant discarded. The cells were resuspended in 1 mL of 0.9 M sorbitol, 0.1M EDTA (pH 7.5). 60 µL of zymoliase (1 U/µL) were added and the cells were incubated for 1 hour at 37 °C. After centrifugation at 2300 rcf for 5 min and discarding the supernatant, the spheroplasts were resuspendend in 1 mL of a 50 mM TrisHCl (pH 8.0), 10 mM EDTA solution. 30 µL of 10% sodium dodecyl sulphate (SDS) were then added to the suspension and it was incubated at 65 °C during 30 min. The suspension was chilled on ice for 1h following the addition of 250 µL 5M potassium acetate. A centrifugation of 9300 rcf for 10 min was performed in order to obtain the DNA containing supernatant. 1.5 mL of ethanol absolute at 4 °C was added, mixed and discarded

after centrifugation at 4500 rcf. The pellet was then washed twice with 70% ethanol and let to dry. The cells were resuspended in 200 μ L of TE (10 mM TrisHCl (pH 8.0), 1 mM EDTA solution) and incubate with RNase (1 mg/mL) for 30 min at 37 °C. A final centrifugation of 15 min at 9300 rcf was performed and the supernatant stored at -20 °C.

2.2.4 Agarose gel electrophoresis

Gels used were 1% (w/v) agarose in 1X TAE (40 mM Tris-base, 5.71% (v/v) glacial acetic acid, 50 mM EDTA) buffer. Electrophoresis was performed at 200V, non-limiting amperage and using 1X TAE running buffer. “*GeneRuler 1 kb DNA Ladder, ready-to-use*” was used as molecular weight marker and DNA samples were prepared with 6X loading buffer (0.25% (w/v) Bromophenol Blue and 30% glycerol). DNA staining was achieved via fluorescence by either incubating post-electrophoresis gels in a 2 μ g/mL solution of ethidium bromide or by adding 2 μ L of a 1:400 diluted solution of MG04 - Midori Green Advance, 1ml, 20,000X to loading solutions (6 μ L total). DNA bands visualization and image capture were performed using a VWR GenoSmart (USB) transilluminator.

2.2.5 PCR conditions

PCR with Taq polymerase was used to amplify genes and TPs, and as confirmation of positive transformants (colony PCR). All PCRs reactions used either a Bio-Rad T100™ Thermal Cycler or a VWR DOPPIO Thermal Cycle r with dual 48 well blocks. Taq PCR solutions were prepared as described in table 2 and had a final volume of either 10 μ L (when the conditions were being tried for the first time or for colony PCR), or 50 μ L (when the conditions were already known to work and a large amount of PCR product was required). Volume of template solution was usually 10% of the total, however it was fluctuated between 1% and 30% depending on template concentration and possible existence of contaminants on template solution. All Taq PCRs used a final extension step of 72 °C for 10 min, and almost all used an initial denaturation step of 95 °C for 10 min. As for the cyclic conditions, denaturation temperature was 95 °C for 30s. Annealing lasted for 30 s and T_A was usually determined using “WebPCR” online tool, although there were situations where temperature needed to be empirically optimized. This was due to lack of PCR product under the theoretically ideal conditions, primer dimer competition was usually the probable cause. Extension temperature was 72°C and lasted for 1 min per nucleotide kilobase pair (kbp) of the desired product. Two PCR strategies were used in order to tackle long tailed primers: 35 cycles with the T_A of the primer excluding the tail; First 10 cycles

with the T_A of the primer excluding the tail, and the last 25 cycles with the T_A of the entire primer. For each PCR reaction, the strategy that resulted in most PCR product and least primer dimer was chosen. All primers used are represented in table 3

Table 2. Taq PCR solutions used in this work (without template)

Reagents	Concentration
10X Taq buffer	1X
dNTPs	0.2 mM
5' Primer	1 μ M
3' Primer	1 μ M
Taq DNA polymerase	0.025 U/ μ L
MgCl₂	2 mM
Ultrapure water	-

Table 3. Primers used in this work.

Primer number	Primer sequence (5'→3')
564	tcgtccactccggttccagaccacg
567	GTcggctgcaggctcactagtgag
568	GTGCcatctgtgcagacaaacg
577	gttctgatcctcgagcatcttaagaattc
578	Gttcttgtctcattgccacattcataagt
586	CTCCTCTCTCAAGAAGCAGC
698	ACCTGGCACTTCAATGTATTG
775	gcggccgctgacTTAAAT
778	ggtaaataccggatTAATTAA
781	GCCAGGTTGCCACTTTCTCACTAGTGACCTGCAGCCCACa tgcgactgcaattgaggacact
782	TAAATCCGGATATCCTGATGCGTTTGTCTGCACAGATGACT cacaacccttgagcagctca
967	AAatcctgatgcgtttgtctgcacagatggCACCTACGGTT GAACCACA
968	tgcccacttttctcactagtgacctgcagccgacAAATGGCG

	TCTTCGTCGT
969	AAatcctgatgcgtttgtctgcacagatggCACTTACAAAC ACAATTTAATCTGT
970	tgcccactttctcactagtgacctgcagccgacAAATGGAC GCTTCTATGATTA
971	AAatcctgatgcgtttgtctgcacagatggCACTCAGGCGA AGCTGGGG
972	tgcccactttctcactagtgacctgcagccgacAAATGGCT TCAATATCGC
973	AAatcctgatgcgtttgtctgcacagatggCACTTAATTTG TGTTCAAAGGA
974	tgcccactttctcactagtgacctgcagccgacAAATGGAA AAATCGTGGT
1045	tgcccactttctcactagtgacctgcagccgacaaatgtct cggctcaagaaag
1046	tgcccactttctcactagtgacctgcagccgacaaatgtgc agtgggtggtg
1047	tgcccactttctcactagtgacctgcagccgacaaatgtca gctgaaggaaag
1048	aatcctgatgcgtttgtctgcacagatggcacttatttgt acaattcatccatacc
1049	acctttagaaccagcaccgtcaccatttgtgttcaaaggaa aa
1050	acctttagaaccagcaccgtcaccggcgaagctgggggta
1051	acctttagaaccagcaccgtcacccaacacaatttaattct gt
1052	acctttagaaccagcaccgtcaccggttgaaccacaaaca ga
1053	aacacaaatggtgacggtgctggttctaaagggtgaagaatt attcac
1054	agcttcgccggtgacggtgctggttctaaagggtgaagaatt attcac
1055	ttgtgtttgggtgacggtgctggttctaaagggtgaagaatt

	attcac
1056	gttcaaccgggtgacgggtgctggttctaaaggtgaagaatt attcac
1057	tgcccacttttctcactagtgacctgcagccgacaaatgact gaaaaatcgtggttcaatt
1058	tgcccacttttctcactagtgacctgcagccgacAAATGACT GACGCTTCTATGATTA
1059	aactttggtatgcctactcc
1060	cctcttatttttagtggttcttccgg
1061	attgagaagctcaaggaagaattcaa
1062	tggatggtatctggagaagttcgt
1063	tgaaatagagtctgaccataccgg
1064	tgtccttgagctaactaaaagatca
1065	agtgataatctgctcagtgaatcca
1066	tcatgagcagttctgataacacga
1067	catttgatgatgcaccagtactaacc
accD_C->T_fw	aagaatcgagcttttgattgatccgggtacttggaaatcct
accD_C->T_rv	gtaccgggatcaatcaaagctcgattctttctgaactact
ScACC1_fw	cccacttttctcactagtgacctgcagccgacaaATGAGCGA AGAAAGCT
ScACC1_rv	aatcctgatgcgtttgtctgcacagatggcacTTATTTCA AAGTCTTCAACAAT

The presence of constructs in the colonies obtained after transformation was confirmed by colony PCR. Small samples of each colony were taken with a toothpick and rubbed to the bottom of PCR tubes so as to scatter the cells. For yeast, the tubes were microwaved open at 900 watts for 1 min and 30 seconds before PCR so as to effectively lyse cells and allow access to the DNA. Taq PCR solutions (10 μ L) were then added and PCR was performed. Colony PCR was the only PCR where an initial denaturation step of 15 min was used so as to ensure further cellular lysis. Two distinct PCR reactions were performed for each single gene expression cassette in order to verify the presence of either a TP upstream of the gene or a TP downstream of the gene as shown in table 4.

Table 4. Template and primers used for confirmation PCR (usually colony PCR) in this work.

pYPK0 onstructs verified	Portions of plasmid amplified by PCR	Forward primer	Reverse primer
TEF1_CAC1_TDH3; TEF1_CAC1-ps_TDH3	pYPKpw + TEF1 + <i>CAC1</i>	577	1067
	<i>CAC1</i> or <i>CAC1-ps</i> + TDH3 + pYPKpw	1063	578
TDH3_CAC2_PGI1; TDH3_CAC2_RPL5; TDH3_CAC2-ps_PGI1	pYPKpw + TDH3 + <i>CAC2</i> or <i>CAC2-ps</i>	577	1066
	<i>CAC2</i> or <i>CAC2-ps</i> + PGI1 or RPL5 + pYPKpw	1062	578
PGI1_CAC3_FBA1; RPL5_CAC3_FBA1; PGI1_CAC3-ps_FBA1	pYPKpw + PGI1 or RPL5 + <i>CAC3</i> or <i>CAC3-ps</i>	577	1065
	<i>CAC3</i> or <i>CAC3-ps</i> + FBA1 + pYPKpw	1061	578
FBA1_accDin_PDC1; FBA1_accDac_PDC1	pYPKpw + FBA1 + <i>accDin</i> or <i>accDac</i>	577	1064
	<i>accDin</i> or <i>accDac</i> + PDC1 + pYPKpw	1060	578
CAC1_CAC2_CAC3_accDirr; CAC1_CAC2_CAC3_accDac; CAC1-ps_CAC2-ps_CAC3-ps_accDirr; CAC1-ps_CAC2-ps_CAC3-ps_accDac; CAC1-ps_CAC2_CAC3-ps_accDac	pYPKpw + TEF1 + <i>CAC1</i> or <i>CAC1-ps</i>	577	1067
	<i>CAC1</i> or <i>CAC1-ps</i> + TDH3 + <i>CAC2</i> or <i>CAC2-ps</i>	1063	1066
	<i>CAC2</i> or <i>CAC2-ps</i> + PGI1 or RPL5 + <i>CAC3</i> or <i>CAC3-ps</i>	1062	1065
	<i>CAC3</i> or <i>CAC3-ps</i> + FBA1 + <i>accDin</i> or <i>accDac</i>	1061	1064
	<i>accDin</i> or <i>accDac</i> + PDC1 + pYPKpw	1060	578
TEF1_CAC1-yEGFP_TDH3	pYPKpw + TEF1 + <i>CAC1</i>	577	1067
TDH3_CAC2-yEGFP_PGI1	pYPKpw + TDH3 + <i>CAC2</i>	577	1066

PGI1_CAC3-yEGFP_FBA1	pYPKpw + PGI1 + <i>CAC3</i>	577	1065
FBA1_accDac_yEGFP_PDC1	pYPKpw + FBA1 + <i>accDac</i>	577	1064
TEF1_ScACC1_TDH3	pYPKpw + TEF1 + <i>ScACC1</i>	577	698
TEF1_YIACC1_TDH3	pYPKpw + TEF1 + <i>YIACC1</i>	577	564
TEF1_YIACC1_TDH3	pYPKpw + TEF1 + <i>YIACC1</i>	586	578

Phusion DNA polymerase was used for the amplification of genes larger than 4000 bp and solutions were prepared as described in table 5. For these reactions, the initial denaturation step lasted 30 s at a temperature of 98 °C and the final extension step lasted for 10 min at a temperature of 72 °C. In regards to the cyclic conditions, denaturation temperature was 98 °C for 10 s. Annealing lasted for 30 s and T_A was determined using the same tools described for Taq PCRs. The extension temperature was 72°C and lasted for twice of the time suggested in “WebPCR” online tool (Johansson, n.d.). Whenever nonspecific PCR products were present after amplification, the nonspecificity was tackled by use of Touchdown PCR (Korbie & Mattick, 2008). The primer pairs used for every non-colony PCR reaction are indicated in table 6.

Table 5. Phusion PCR solutions used in this work (without template)

Reagents	Concentration
5X Phusion buffer	1X
dNTPs	0.2 mM
5' Primer	1 μM
3' Primer	1 μM
Phusion DNA polymerase	0.025 U/ μL
MgCl₂	2 mM
Ultrapure water	-

Table 6. Template and primers used for non-confirmation amplification in this work.

Template	PCR product	Forward primer	Reverse primer
Arabidopsis Thaliana cDNA	CAC1	968	967
	CAC2	970	969
	CAC3	972	971
	accDin	974	973
	accDF	1057	accD_C->T_rv
	accDT	accD_C->T_fw	973
	CAC1-ps	1047	967
	CAC2-ps	1046	969
	CAC3-ps	1045	971
	CAC1linker	968	1052
	CAC2linker	1058	1051
	CAC3linker	972	1050
	accDinlinker	1057	1049
pUG35	yEGFPCAC1	1056	1048
	yEGFPCAC2	1055	1048
	yEGFPCAC3	1054	1048
	yEGFPaccDin	1053	1048
<i>Saccharomyces cerevisiae</i> genomic DNA	<i>ScACC1</i>	ScACC1_fw	ScACC1_rv
<i>Yarrowia lipolytica</i> genomic DNA	<i>YIACC1α</i>	781	505
	<i>YIACC1β</i>	504	782
pYPKa_Z_TEF1	TEF1	577	567
pYPKa_Z_TDH3	TDH3		
pYPKa_Z_PGI1	PGI1		
pYPKa_Z_FBA1	FBA1		
pYPKa_Z_RPL5	RPL5		
pYPKa_E_TDH3	TDH3	568	578
pYPKa_E_PGI1	PGI1		

pYPKa_E_FBA1	FBA1		
pYPKa_E_PDC1	PDC1		
pYPKa_E_RPL5	RPL5		
pYPKO_TEF1_CAC1_TDH3	TEF1_CAC1_TD H3	577	778
pYPKO_TDH3_CAC1-ps_PGI1	TDH3_CAC2- ps_PGI1		
pYPKO_TDH3_CAC2_PGI1	TDH3_CAC2_P GI1	775	778
pYPKO_TDH3_CAC2_RPL5	TDH3_CAC2_RP L5		
pYPKO_TDH3_CAC2-ps_PGI1	TDH3_CAC2- ps_PGI1		
pYPKO_PGI1_CAC3_FBA1	PGI1_CAC3_FB A1		
pYPKO_RPL5_CAC3_FBA1	RPL5_CAC3_FB A1		
pYPKO_PGI1_CAC3-ps_FBA1	PGI1_CAC3- ps_FBA1		
pYPKO_FBA1_accDin_PD C1	FBA1_accDin_P DC1	775	578
pYPKO_FBA1_accDac_PD C1	FBA1_accDac_P DC1		

2.2.6 Single gene expression cassettes construction

Single gene expression constructs are listed in table 1, in 12th to 23rd rows. *CAC1*, *CAC2*, *CAC3* and *accD* coding sequences (CDS) were amplified from cDNA of *Arabidopsis thaliana* kindly provided by Romulo Sobral and Manuela Costa (Department of Biology, University of Minho, Portugal). *Saccharomyces cerevisiae ACC1* (*ScACC1*) was amplified from genomic DNA extracted from *S. cerevisiae* CEN.PK102-3A. *Yarrowia lipolytica ACC1* (*YIACC1* - YALIOC11407g) was amplified from

genomic DNA extracted from *Y. lipolytica* PYCC 3347. The primers used for these amplifications were tailed by 35 bp (forward primers) or 33 bp (reverse primers). The forward primers grant homology with the 33 bp upstream of restriction site *Ajl* in pYPKa (Pereira et al., 2016) while the reverse primers provide homology with the 33 bp downstream of *Ajl*. The forward primer's tail is 35 bp long because two adenines were added before the ATG codon as a way to increase similarity of the sequence to the yeast Kozac consensus sequence and increase translation (Nakagawa et al., 2008). In the case of genes CAC2 and accD used slightly different primers that added a codon after ATG that is known to increase polypeptide half-life in the cytosol (Bachmair & Varshavsky, 1989). For each of the genes CAC1, CAC2 and CAC3, two versions were amplified, one of the complete gene (represented as CAC1, CAC2 and CAC2), and one of the gene without the signal peptides. This was achieved by using forwards primers that pair with the sequence of the template immediately after the signal peptide sequences. These primers also added an ATG codon to the beginning of the gene in order to allow initiation of translation and, when necessary, added a codon after ATG that is known to increase polypeptide half-life in the cytosol (Bachmair & Varshavsky, 1989).

The TPs used in this study were obtained by PCR from plasmids that already contained them. These plasmids were named pYPKa_Z_TP when the TP was cloned in the restriction site *Zral* of pYPKa or pYPKa_E_TP when it was cloned in the restriction site *EcoRV*, where "TP" is replaced by the TP specific name (Pereira et al., 2016).

Zral cloned TPs were amplified by primers 577 and 567 (table 6). This results in pYPKa_Z_TP PCR products having 5' homology with 124 bp upstream of the pYPKpw restriction site *EcoRV* and containing at the 3' end the portion upstream of pYPKa restriction site *Ajl* to which the forward primer tail of the gene PCR products grant homology (Figure 3).

EcoRV cloned TPs were amplified by primers 568 and 578 (table 6). This results in YPKa_E_TP PCR products possessing at the 5' end the portion downstream of pYPKa restriction site *Ajl* to which the reverse primer tail of gene the PCR products gives homology, and being homologous at the 3' end with 241 bp downstream of pYPKpw restriction site *EcoRV* (Figure 3).

The PCR product of each gene was co-transformed in *Saccharomyces Cerevisiae* together with corresponding TP PCR products and pYPKpw previously digested with *EcoRV* and treated with Shrimp Alkaline Phosphatase (SAP) so as to prevent empty plasmid self-ligation. The fragments were joined by the yeast itself through homologous recombination. This process was performed in the CEN.PK 113-5D strain in the case of *Arabidopsis thaliana* ACC genes. In the case of the *ScACC1* and *YIACC1*

constructs, the Δ Acc Tet strain was used instead so as to allow screening for functional ACC by growth overnight on solid YPD Tet, a medium that inhibits expression of this strain's endogenous ACC.

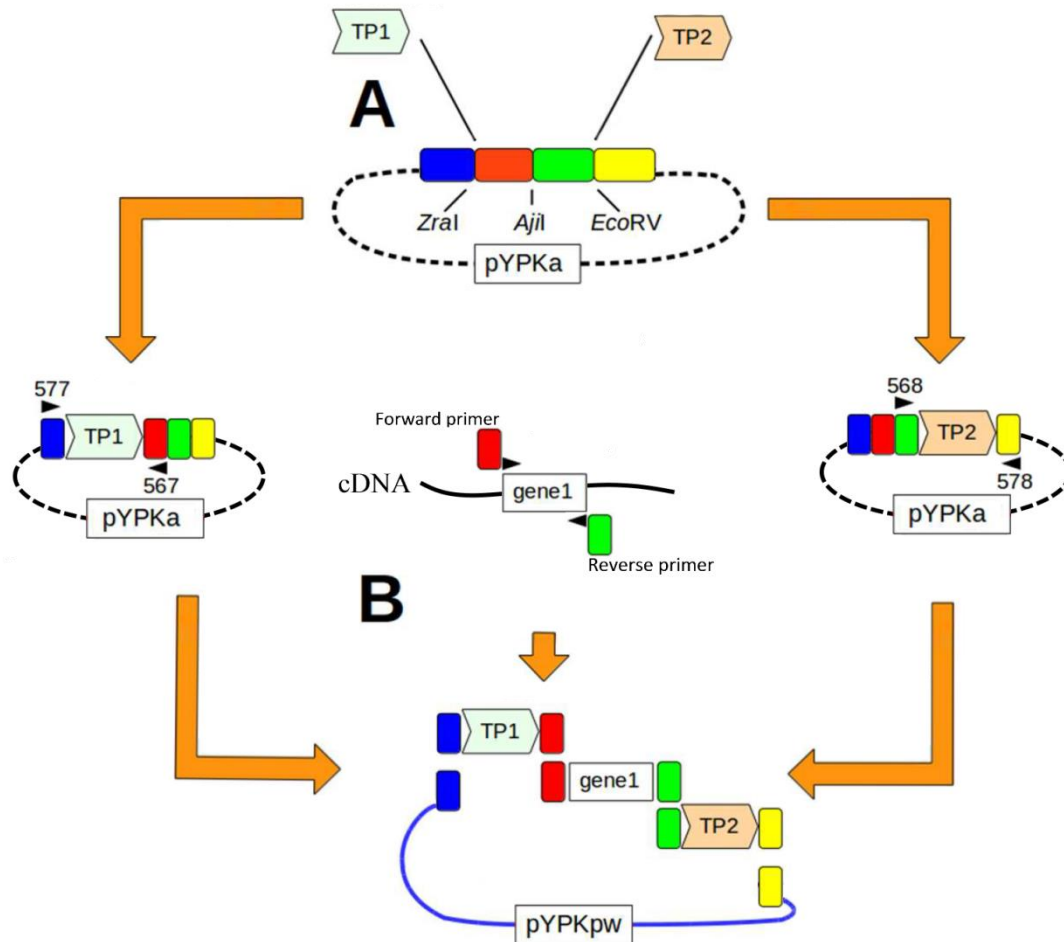


Figure 3 - Schematic representation of TP_Gene_TP assembly. **A**, relative positions of restriction sites Zral, Ajil and EcoRV in the pYPKa plasmid. The blue box represents the sequence upstream of Zral in pYPKa that shares homology with 124 bp upstream of the pYPKpw restriction site EcoRV. The red box represents the sequence between Zral and Ajil, and the green box represents the sequence between Ajil and EcoRV. The yellow box represents the sequence downstream of EcoRV in the pYPKa plasmid that shares homology with 241 bp downstream of the pYPKpw restriction site EcoRV. **B**, PCR with the appropriate primers generates PCR products that share homologous portions between themselves and the linearized

2.2.7 Activation of accD gene

The *A. thaliana accD* gene is subject to RNA editing that changes the cytosine in the position 794 to Uracil. This converts the original Ser codon to Leu and is required for the CT activity of the β -CT subunit (Salie & Thelen, 2016). Since the sequence obtained from cDNA was the inactive form of accD (accD_{in}), it was necessary to change this codon if any activity was to be expected. Primers accD_C-

>T_{rv} and accD_C->T_{fw} were used in order to replace this cytosine with a thymine. The PCR of accD by use of primers 974 and accD_C->T_{rv} originates fragment accDF, and PCR by primers accD_C->T_{fw} and 973 originates fragment accDT. These fragments are capable of originating the active form of *accD* (*accDac*) by homologous recombination when cloned together in *Saccharomyces cerevisiae*.

2.2.8 *Saccharomyces cerevisiae* transformation

Cell culture was grown overnight in 10 mL YPD medium. This culture was used to initiate a 0.2 OD₆₄₀ culture that was left to grow until it reached 0.8-1 OD₆₄₀. At this OD₆₄₀ the cells were centrifuged 2 min at 4500 rcf and the pellet was resuspended in ultra-pure water and divided into aliquots in microcentrifuge tubes. These were centrifuged at 2300 rcf and the different 360 µL transformation solutions (33,3% (w/v) polyethylene glycol (PEG); 0.1 M Lithium acetate; 0.28 mg/mL salmon sperm DNA; 100-1000 µg DNA to be transformed) were added to the different pellets. Following vortex, the resuspensions were incubated at 30 °C for 30 min. Cells were then kept 40 min at 42°C in a water bath and centrifuged 2 min at 2300 rcf. Each pellet was resuspended in 100 µL of water and the cells were plated in either SD URA⁻ (CEN.PK 113-5D or ΔAcc Tet) or defined medium (CEN.PK 113-5D). The cells were incubated at 30 °C for 3 days and positive clones were confirmed by colony PCR. The constructs transformed in ΔAcc Tet were the TP1_*ScACC1*_TP2, the TP1_*YIACC1*_TP2 and the MS-ACC gene cluster constructs because these were expected to grant ACC activity. After transformation, the ΔAcc Tet clones growing in SD URA⁻ plates were plated to YPD Tet agar medium. The ΔAcc Tet cells capable of growing on YPD Tet are likely to contain a plasmid whose construct endows the cell with ACC activity.

2.2.9 Gel extraction of DNA

Yeast enhance Green fluorescent protein (yEGFP) PCR products were separated from template and other PCR debris, via normal agarose gel electrophoresis followed by gel extraction. Since yEGFP was amplified from pUG35 and this plasmid is capable of complementing uracil auxotrophy, the presence of this plasmid in the DNA used for yeast transformation could result in false positive colonies. After electrophoresis the DNA band corresponding to the desired PCR product was excised from the gel by use of a surgical blade. A 500 µL microcentrifuge tube was punctured at the bottom by a 22G syringe needle and a piece of cotton was placed at the bottom so as to create ~4 mm cushion filter. The excised gel was then placed on the cushion filter and the 500 µL microcentrifuge tube was placed

in a 1.5 mL microcentrifuge which was centrifuged at 2300 rcf for 5 min. The 1.5 mL microcentrifuge containing the purified yEGFP PCR product was stored at -20 °C (Sun et al., 2012).

2.2.10 yEGFP fusion protein expression cassettes construction

yEGFP fusion protein expression constructs are listed in table 1, in 24th to 28th rows. While CAC1 and CAC3 genes were amplified using the same forward primers as in TP_Gene_TP construction, CAC2 and accD used slightly different primers that added a codon after ATG that is known to increase polypeptide half-life in the cytosol (Bachmair & Varshavsky, 1989). All four genes were amplified using different reverse primers. These new reverse primers encode a linker that will serve as a bridge between each single MS-ACC subunit and yEGFP. This tail is ended by a 9 bp sequence that provides homology to the beginning of the *yeGFP* gene with the exception of the start codon. The primers used in this work possess the linker encoding sequence of primer F5 described in Sheff & Thorn, 2004. *yEGFP* was amplified from pUG35 (Güldener and Hegemann, <http://mips.gsf.de/proj/yeast/info/tools/hegemann/gfp.html>) using forward primers that exclude the *yEGFP* start codon and grant homology to the linker sequence and the last 9 bp of CAC1, CAC2, CA3 or accD. The reverse primer used for GFP amplification is tailed by a 33 bp sequence that provides homology with the 33 bp downstream of *Ajl* in pYPKa. TPs were amplified using the same primers as in single gene expression cassettes construction. The fragments were also joined and inserted in the pYPKpw plasmid in the same way and using the same *Saccharomyces cerevisiae* strain.

2.2.11 Competent *E. coli* and transformation

A 2 mL LB medium culture was inoculated from a single *E. coli* XL1 Blue or BL21(DE3) colony and grown overnight. This culture was used to inoculate 200 mL of LB medium which was incubated at 37 °C until OD₆₀₀ reached 0.35-0.4. The culture was then chilled for 30 min at 4 °C. The cells were centrifuged at 3000 rcf for 15 min at 4 °C, the supernatant discarded and the pellet resuspended in 100 mL 100 mM MgCl₂. The suspension was centrifuged at 2000 rcf for 15 min at 4 °C. After discarding the supernatant, the pellet was resuspended in 80 mL 100 mM CaCl₂ and chilled for 20 min at 4 °C. The cells were harvested by centrifugation at 2000 rcf for 15 min at 4 °C, the supernatant discarded and the pellet resuspended in 20 mL 85 mM CaCl₂, 15% glycerol (v/v). The solution was centrifuged at 1000 rcf for 15 min at 4 °C. The supernatant was discarded and the cells were

resuspended in 400 μ L 85 mM CaCl₂, 15% glycerol (v/v). The suspension was then transferred into sterile 1.5 mL microcentrifuge tubes in 50 μ L aliquots and stored at -80°C.

The transformation consisted of thawing the calcium competent cells for 15-30 min. Each stored 50 μ L aliquot is 10 \times concentrated, therefore each aliquot was first divided in 10 aliquots and 45 μ L 85 mM CaCl₂, 15% glycerol (v/v) were added to each. 10 μ L of plasmid DNA was then added to each aliquot and the cells were chilled on ice for 30 min. This was followed by a heat bath at 42 °C for 45s and incubation on ice for 10 min. 950 μ L of LB were then added to each aliquot and the cells were left to recover at 37 °C for 1h. The cells were plated in LB Amp (100mg/L) and incubated for ~16h at 37 °C. The presence of clones containing the desired plasmid was tested by colony PCR.

2.2.12 MS-ACC gene cluster expression plasmids construction

MS-ACC gene cluster expression constructs are listed in table 1, in 29th to 34th rows. TP_Gene_TP cassettes were amplified by using different primers depending on the position of the multiple gene expression construct they would be placed in. The first cassette was amplified by using primers 577 and 778. Amplification with primer 577 provides this cassette with 5' homology with 124 bp upstream of the pYPKpw restriction site *EcoRV*. Second and third cassettes were amplified by using primers 775 and 778. These are small primers (18-20bp) specific to the region immediately flanking the TP_Gene_TP cassette. The last cassette was amplified by using primers 775 and 578. Amplification with primer 578 provides this cassette with 3' homology with 241 bp downstream of the pYPKpw restriction site *EcoRV*.

The fragments were joined and inserted in the pYPKpw plasmid by homologous recombination with the TPs themselves providing the required homology between cassettes. The Δ Acc Tet strain was used for this construction so as to allow screening for functional Multi-subunit ACC (MS-ACC) by growth overnight on solid YPD Tet medium.

2.2.13 Δ Acc Tet growth curves in tetracycline

Cultures of CEN.PK2-1C wild-type, Δ Acc Tet wild-type and Δ Acc Tet cells containing functional *ACC1* constructs or pYPKpw were inoculated in either SC or SD URA- and grown over night. These cultures were used to inoculate YPD Tet medium starting at an OD_{640} of approximately 0.04. OD_{640} measurements were performed every 1 h and 30 min in a span of 48h. Due to the impossibility of following the same inoculums for the entire 48h of growth: one set of inoculums was measured in the time intervals from 0 to 12 h and from 24 to 36 h; the other set was measured in the time intervals from 12 to 24 h and from 36 to 48 h. Growth rates were calculated using the formula shown in Figure 4.

$$\mu = \frac{\ln OD_2 - \ln OD_1}{(t_2 - t_1)}$$

Figure 4 – Growth rate formula. After plotting the growth curve in the exponential growth phase of the data, two points are chosen. OD_1 and t_1 are the OD and time (in hours), respectively, for one of the points. OD_2 and t_2 are the OD and time, respectively, for the other point.

2.3 Protein Biochemistry

2.3.1 Fluorescence microscopy

CEN.PK113-5D cells transformed with TP1_Gene_GFP_TP2 constructs were visualized via fluorescence microscopy in order to assess if the ACC subunits were being expressed and if the signal peptides were targeting the proteins to somewhere other than the cytosol. CEN.PK113-5D cells transformed with pUG35 were used as positive control and non-transformed CEN.PK113-5D were used as negative control. Cell cultures transformed with pUG35 were grown overnight in SD URA- medium without methionine as required in order to prevent inactivation of the MET17/MET25 promoter and allow GFP expression. The other cell cultures were grown overnight in liquid SD URA- medium. 10 μ L of each culture were placed between a microscope slide and a cover slip and the cells were visualized using a Leica DM 5000B microscope.

2.3.2 MCR extraction and SDS-PAGE

The Malonyl-CoA reductase (MCR) coding plasmid pTrc-McrCa (Kroeger et al., 2011) was transformed into competent *E. coli* BL21(DE3). Three starter cultures of 10mL of LB Amp (100 mg/L) medium were inoculated each from a single colony of pTrc-McrCa transformed *E. coli* and grown overnight. These cultures were used to inoculate three 10 mL cultures at 0.05 OD₅₇₈. One 250 mL LB amp culture was also inoculated at this OD₅₇₈ from one of the starter cultures. At 0.6-0.8 OD₅₇₈ MCR expression was induced with 0.5 mM isopropyl β -D-1-thiogalactopyranoside (IPTG). 4 h after induction the 250 mL LB amp culture was centrifuged at 5400 rcf, the supernatant discarded and the pellet resuspended in 25 mL TE. Cells were lysed by sonication at 4 °C in a Bioblock Scientific Vibra-Cell™ Ultrasonic Liquid Processor 75043. Since the MCR gene is originally from a moderate thermophile (*Chloroflexus aurantiacus*) it was possible to purify by heat precipitation of the *E. coli* cell extract for 15 min at 60 °C. Following centrifugation for 1h at 16000 rcf, the MCR containing supernatant was stored at -20 °C. 50 μ L of this extract were mixed with 100 μ L SDS sample buffer (2% SDS (w/v), 2mM β -mercaptoethanol, 4% glycerol (v/v), 0.04M Tris HCl (pH 6.8), 0.01% Bromophenol blue (w/v)) for later analysis via SDS-PAGE (PAGE). The OD₅₇₈ of the 10 mL LB amp cultures was measured at 0h, 2h, 4h and 6h after induction. 1 mL samples were taken at 0h and, together with OD₅₇₈ measurements, were used to calculate the volume the samples at 2h, 4h and 6h would have to be in order to ensure the

same number of cells was present in all samples. The samples were then centrifuged at 16100 rcf, the supernatant discarded and the pellets resuspended in 200 μ L of SDS-PAGE sample buffer. The samples were lysed by heating at 95 $^{\circ}$ C for 15 min and stored at -20 $^{\circ}$ C.

Both the purified cell extract performed 4h after induction and the brute cell extracts taken at different times were resolved on 8% SDS-PAGE polyacrylamide gels. Each 0.75 mm running gel was made using 2.1 mL distilled water, 0.8 mL 40% Acrylamide/Bisacrylamide (Bio-Rad), 1 mL 1.5 M Tris-HCl (pH 8.8), 40 μ L 10% (w/v) SDS, 40 μ L 10% (w/v) ammonium persulfate (APS), 4 μ L N,N,N',N'-Tetramethylethylenediamine (TEMED). The mixture was poured between the assemble plates and the gel overlaid with distilled water. After polymerization (\sim 1 h), the water was poured off and the 6% stacking gel was poured on top of the running gel. Each stacking gel was made using 1.16 mL distilled water, 0.3 mL 40% Acrylamide/Bisacrylamide, 0.5 mL 0.5 M Tris-HCl (pH 6.8), 20 μ L 10% (w/v) SDS, 20 μ L 10% (w/v) ammonium persulfate (APS), 2 μ L N,N,N',N'-Tetramethylethylenediamine (TEMED). The gels were then sealed with combs and let to polymerize for approximately 1 h. The molecular weight marker used was Bio-Rad Precision Plus Protein™ Unstained Standards. Gels were run at 100 V for 1 h followed by 140 V for 2 h in Tris-Glycine-SDS PAGE buffer (24.8 mM, 1.44% glycine, 1% SDS). After electrophoresis, the gels were washed with acidified water (0.3% HCl) for 10 min. This was followed by incubation overnight in a solution of Coomassie Brilliant Blue G250 (0.008% (w/v) Coomassie G250, acidified water (0.3% HCl)). The gels were then incubated in a solution of acidified water (0.3% HCl) that was changed regularly until complete destaining of the background.

3. RESULTS AND DISCUSSION

3.1 Confirmation of ACC Tet as a ACC activity testing strain

The Δ Acc Tet strain was previously created by our group in unpublished work. In this strain, the native *ACC1* promoter is replaced by a cassette that regulates translation of the target mRNAs by inserting a tetracycline aptamer with strong binding affinity for tetracycline into the 5'UTRs (Kötter et al., 2009). This means that the essential *ACC1* gene (Tehlivets et al., 2007) will not be expressed in a medium containing tetracycline and the yeast will not grow. In order to verify if this conditional *ACC1* null mutation of Δ Acc Tet can be complemented by a plasmid, the native *ACC1* expression construct pYPK0_TEF1_*ScACC1*_TDH3 was created and expressed in this strain. The tailed *ScACC1* fragment (6768 bp) was successfully amplified from *S. cerevisiae* CEN.PK102-3A genomic DNA (primers ScACC1_fw and ScACC1_rv). Even though the amplification of a nonspecific fragment (~2500 bp) could not be prevented, touchdown PCR (Korbie & Mattick, 2008) was successful in diminishing the concentration of this fragment (Figure 5). As expected, Δ Acc Tet containing pYPK0_TEF1_*ScACC1*_TDH3 was able to grow on solid YPD Tet medium (Figure 6). The presence of this construct was confirmed by PCR (Figure 7).

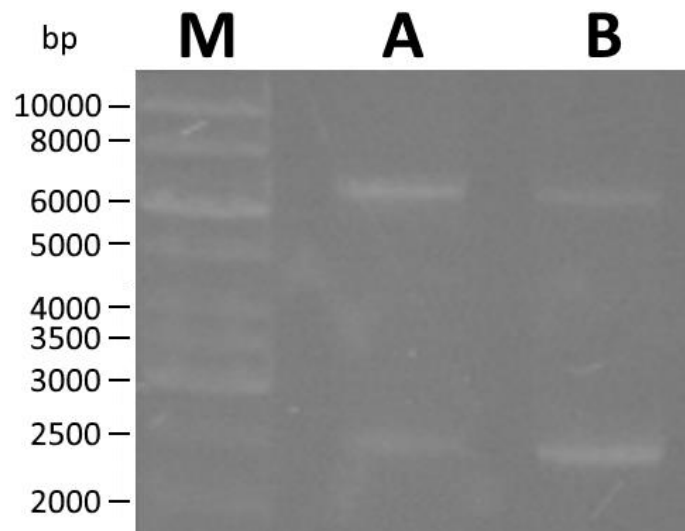


Figure 5 – Electrophoresis agarose gel of phusion polymerase PCR amplification of *ScACC1*. **A**, the products from touchdown PCR: 10 cycles with T_A decreasing 1°C after each cycle, with T_A starting at 66°C. The 25 remaining cycles used a T_A of 56° C. **B**, the products from the non-touchdown PCR conditions with the best results (annealing at 59 °C). No negative control was used due to limited availability of phusion polymerase. **M** is the molecular weight marker.

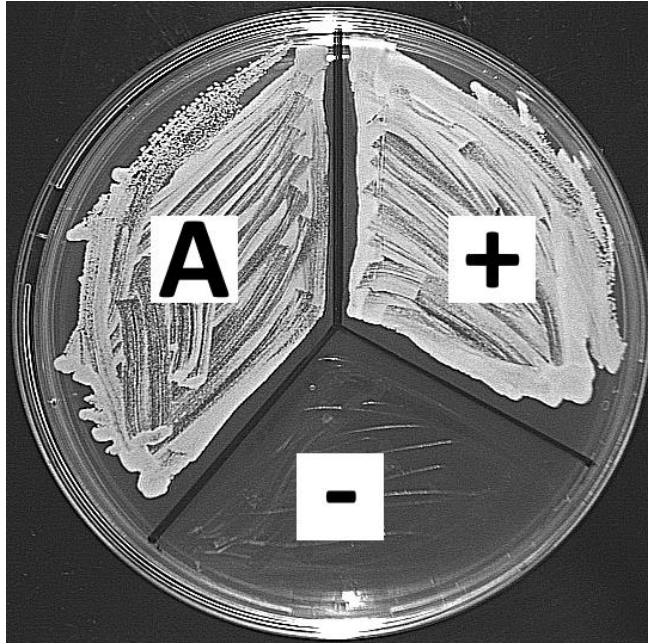


Figure 6 – Complementation of a conditional *ACC1* null mutation by pYPK0_TEF1_ScACC1_TDH3 on solid YPD Tet medium. **A**, ΔAcc Tet containing pYPK0_TEF1_ScACC1_TDH3. **+**, CEN.PK2-1C was used as positive control. **-**, Empty ΔAcc Tet is used as negative control.

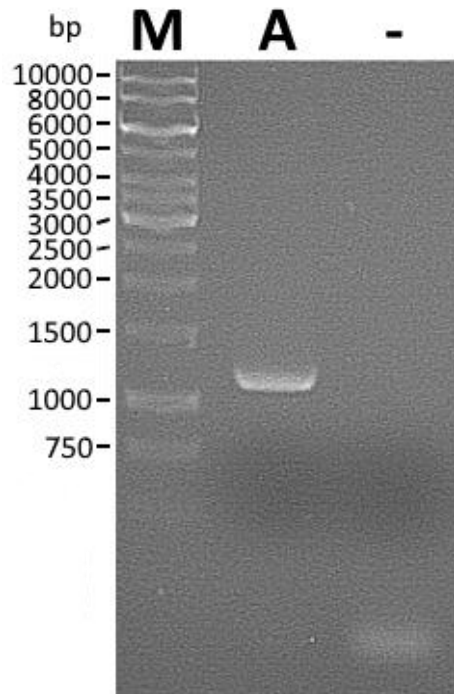


Figure 7 – Electrophoresis agarose gel of PCR verification of the pYPK0_TEF1_ScACC1_TDH3 construct. **A**, amplification of the 1176 bp fragment encompassing TEF1 and a small portion of *ScACC1* by use of primers 577 and 698. **-**, an equal PCR reaction without template was used as negative control. **M**, molecular weight marker.

3.2 Heterologous expression of *Arabidopsis thaliana* MS-ACC in *S. cerevisiae*

A. thaliana accumulates around 38% of oil by dry weight in its seeds (O'Neill et al., 2003). This value is comparable to the amount found in some oleaginous yeasts (Beopoulos et al., 2009). The MS-ACC of this plant is thus an alluring choice for heterologous expression when one is attempting to increase malonyl-CoA production in *S. cerevisiae*. The plastidic ACC of *A. thaliana* is coded by 5 genes: *CAC1A* (At5g16390) codes for the BCCP subunit 1 (BCCP1); *CAC1B* (At5g15530) codes for the alternative version, BCCP subunit 2 (BCCP2); *CAC2* (At5g35360) codes for the BC subunit; *CAC3* (At2g38040) codes for the CT- α subunit; *accD* (AtCg00500) codes for the CT- β subunit (Salie & Thelen, 2016). *CAC1A* and *CAC1B* are paralogs and only one BCCP type is needed for ACC1 activity. In fact, *CAC1A* but not *CAC1B* is needed for survival in *A. thaliana* (X. Li et al., 2011). For this reason, only the genes *CAC1A*, *CAC2*, *CAC3* and *accD* were chosen. In the present work, *CAC1A* is called by its alternative name of *CAC1* as used in its Genbank database entry.

3.2.1 Complete gene MS-ACC expression

The complete CDSs of the 4 *A. thaliana* MS-ACC genes were successfully amplified from *A. thaliana* cDNA (Figure 8).

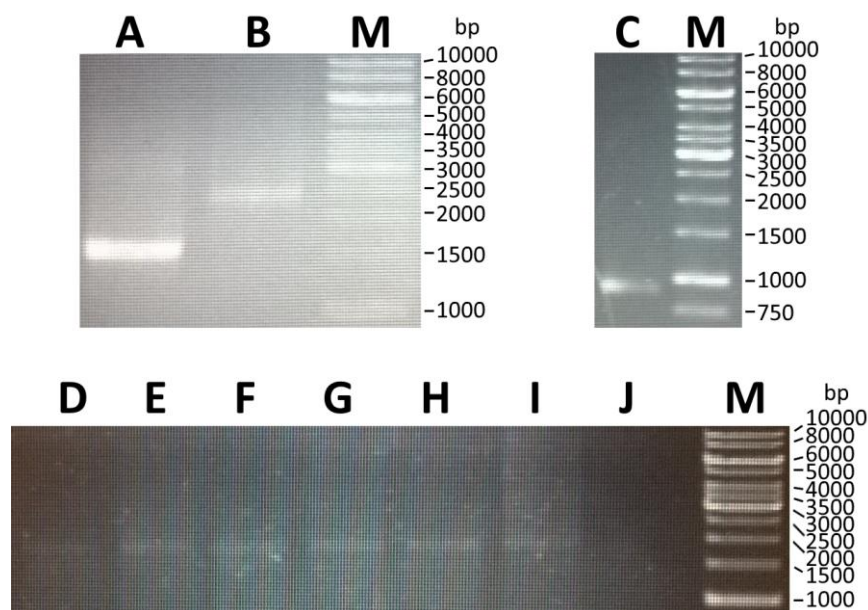


Figure 8 - Electrophoresis agarose gel of PCR amplification of fragments *CAC1*, *CAC2*, *CAC3* and *accDin*. **A** (1467 bp), *accDin* amplification at a T_A of 52 °C (primers 974 and 973). **B** (2378 bp), *CAC3* amplification at a T_A of 59 °C (primers 972 and 971). **C** (911 bp), *CAC1* amplification at a T_A of 55 °C primers (968 and 967). **D**, **E** and **F** (1736 bp), *CAC2* amplification at a T_A of 60 °C. **G**, **H** and **I** (1736 bp), *CAC2* amplification at a T_A of 62 °C (primers 970 and 969). **J**, failed try at *CAC2* amplification at a T_A of 62 °C, by using a PCR reaction with a primer concentration of 0.5 μ M instead of the usual 1 μ M. **M**, molecular weight marker.

Screening for clones with correctly assembled single gene expression cassettes was done via two colony PCRs per construct (Figures 9). One PCR product spans part of the gene and the entire upstream TP (primer 577 as forward and a gene specific primer as reverse: either 1067, 1066, 1065 or 1064), the other spans part of the gene and the entire downstream TP (primer 578 as reverse and a gene specific primer as forward: either 1063, 1062, 1061 or 1060). In regards to the pYPK0_TDH3_CAC2_PGI1 construct, the amplification of the fragment encompassing the downstream TP (2207 bp) was particularly challenging. One possible reason for this could lie in the tendency of yeast colony PCR to produce false negatives. The larger size of this fragment could further exacerbate this problem (Azevedo et al., 2017).

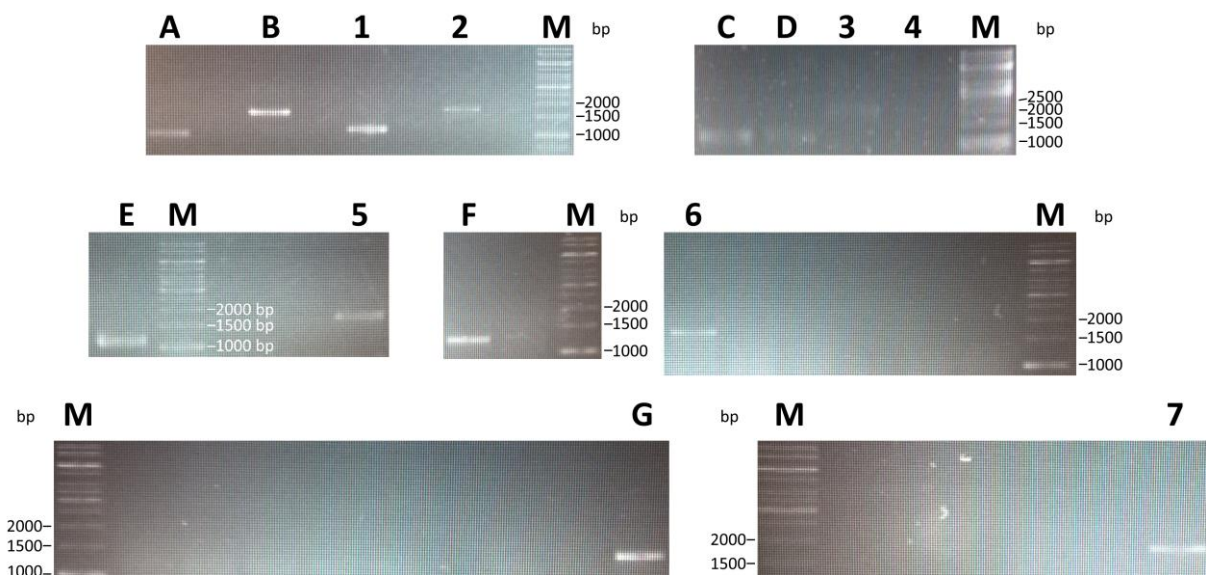


Figure 9 – Electrophoresis agarose gel of colony PCR verification of MS-ACC unaltered single gene expression constructs. Letters are colony PCRs that verify the presence of gene and upstream TP. Numbers are colony PCRs that verify the presence of the gene and downstream TP. All wells with no band are colony PCRs where no amplification occurred. **A** (1036 bp) and **1** (1138 bp), colony PCRs of a correctly assembled pYPK0_TEF1_CAC1_TDH3 construct. **B** (1626 bp) and **2** (1735 bp), colony PCRs of a correctly assembled pYPK0_PGI1_CAC3_FBA1 construct. **C** (1216 bp) and **3** (2207 bp), colony PCRs of a correctly assembled pYPK0_TDH3_CAC2_PGI1 construct. **D** (1216 bp) and **4**, pYPK0_TDH3_CAC2_PGI1 colony PCRs that confirmed the presence of gene and upstream TP, but not of downstream for a specific clone. **E** (1087 bp) and **5** (1694 bp), colony PCRs of a correctly assembled pYPK0_FBA1_accDin_PDC1 construct. **F** (1216 bp) and **6** (1709 bp), colony PCRs of a correctly assembled pYPK0_TDHR_CAC2_RPL5 construct. **G** (1128 bp) and **7** (1735 bp), colony PCRs of a correctly assembled pYPK0_RPL5_CAC3_FBA1construct. **M**, molecular weight marker.

Expression cassettes were successfully amplified (Figure 10) and used for the assembly of constructs pYPK0_CAC1_CAC2_CAC3_accDin and pYPK0_CAC1_CAC2_CAC3_accDin_(PGI1->RPL5) via homologous recombination in ΔAcc Tet. All cassettes used for the assembly of the pYPK0_CAC1_CAC2_CAC3_accDin construct were confirmed via sequencing. This was not the case for cassettes TDH3_CAC2_RPL5 and RPL5_CAC3_FBA1 used for pYPK0_CAC1_CAC2_CAC3_accDin_(PGI1->RPL5) construct assembly.

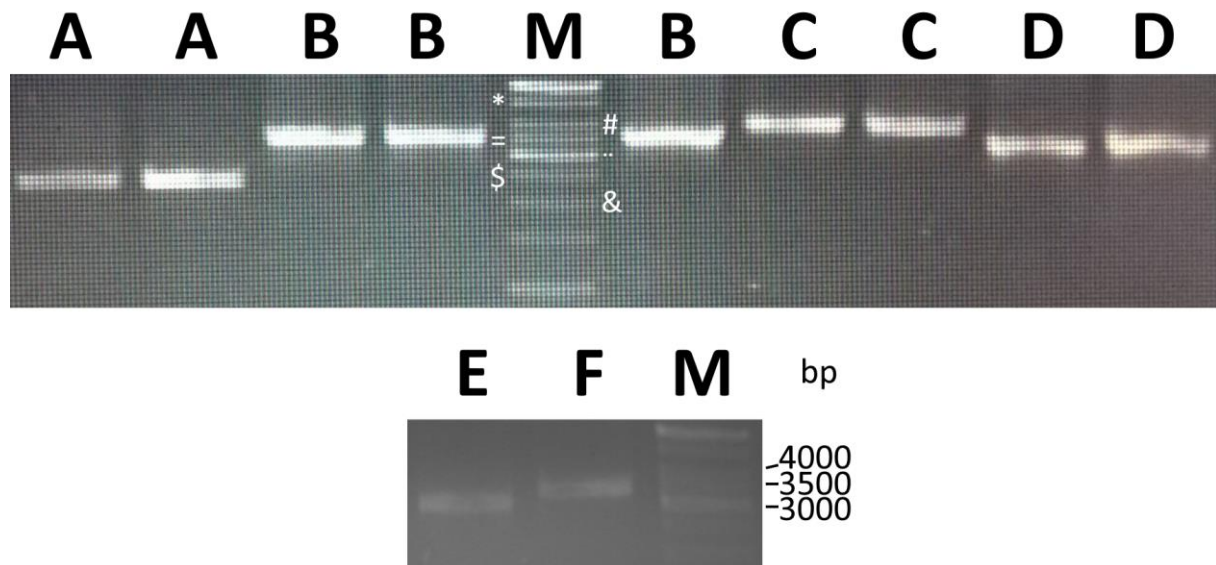


Figure 10 – Electrophoresis agarose gel of MS-ACC single gene expression cassette amplification. **A** (2412 bp), TEF1_CAC1_TDH3 amplification. **B** (3501 bp), TDH3_CAC2_PGI1 cassette amplification. **C** (4075 bp), PGI1_CAC3_FBA1 cassette amplification. **D** (3470 bp), FBA1_accDin_PDC1 cassette amplification. **E** (3003 bp), TDHR_CAC2_RPL5 amplification. **F** (3577 bp), RPL5_CAC3_FBA1 cassette amplification. **M**, molecular weight marker. Relevant molecular weight marker bands: * (5000 bp); # (4000 bp); = (3500 bp); .. (3000 bp); \$ (2500 bp); & (2000 bp).

ΔAcc Tet clones containing either of the MS-ACC gene cluster constructs was unable to grow on solid YPD Tet (Figure 20). pYPK0_CAC1_CAC2_CAC3_accDin assembly was confirmed by colony PCRs: two of these used the same primers as the single expression gene verification PCRs. The rest used gene specific primers to amplify portions of two adjacent genes together with the TP between the them (Figure 11).

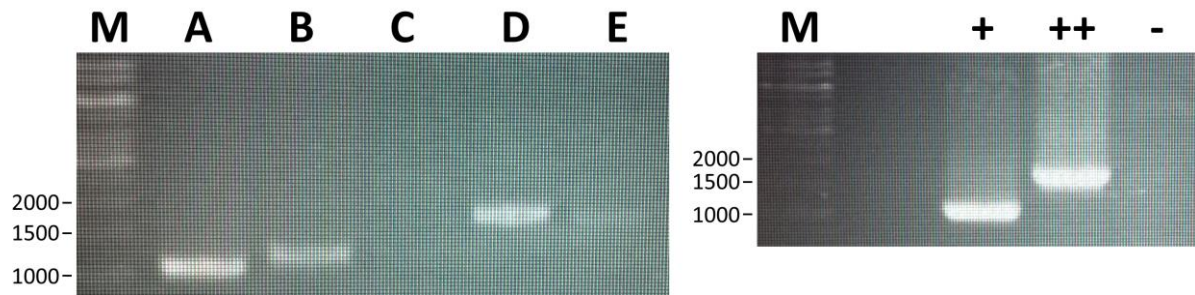


Figure 11 – Electrophoresis agarose gel of colony PCR verification of correct pYPK0_ *CAC1_CAC2_CAC3_accD* assembly. **A** (1036 bp), PCR that verifies the presence of TEF1 upstream of *CAC1* (primers 577 and 1067). **B** (1179 bp), PCR that verifies the presence of *CAC2* downstream of *CAC1* with TDH3 in the middle of the 2 genes (primers 1063 and 1066). **C**, failed PCR verification of *CAC3* as being downstream of *CAC2* with PGI1 in the middle of the 2 genes (primers 1062 and 1065). **D** (1715 bp), PCR that verifies the presence of *accD* downstream of *CAC3* with FBA1 in the middle of the 2 genes (primers 1061 and 1064). **E** (1694 bp), PCR that verifies the presence of PDC1 downstream of *accD* (primers 1060 and 578). **+** (1036 bp), the amplification of the fragment encompassing part of *CAC1* and TEF1 from a previously confirmed pYPK0_TEF1_ *CAC1*_TDH3 was used as a positive control (primers 577 and 1067). **++** (1138 bp), the amplification of the fragment encompassing part of *CAC1* and TDH3 from a previously confirmed pYPK0_TEF1_ *CAC1*_TDH3 was used as other positive control (primers 1063 and 578). **-**, a PCR reaction without template but with primers 1062 and 1065 was used as negative control. **M**, molecular weight marker.

3.2.2 yEGFP fusion proteins expression

A. thaliana genes *CAC1*, *CAC2* and *CAC3* contain sequences coding for signal peptides. Signal peptides are short peptide sequences found at the N-terminus that mediate the targeting and translocation of proteins across membranes (Choo et al., 2009). *accD* does not possess a signal peptide coding sequence. This is probably due to the fact that this gene is coded in the plastid, which means that a plastidic targeting peptide is not needed. Some signal peptides have been shown to work across species (Al-Qahtani et al., 1998). It is, therefore, possible that the presence of these signal peptides could be redirecting some of the MS-ACC subunits to cellular compartments other than the cytosol in *S. cerevisiae*. This would result in no malonyl-coA production since all subunits are needed for there to be ACC activity. In order to investigate this hypothesis, yEGFP fusion protein expression constructs were created for each MS-ACC gene. The expression of these yEGFP fusion proteins in *S. cerevisiae* should enable the visualization of the overall intracellular distribution of MS-ACC subunits. MS-ACC genes were successfully amplified from cDNA using primers containing a sequence that encodes a linker (Figure 12). A linker is a peptide sequence that can be used to connect two proteins, providing distance between the two so that the resulting fusion protein retains the native conformation

and function of each of the proteins that comprise it (Xiaoying Chen et al., 2013). The clones where this constructs were assembled were screened via colony PCR of the region encompassing the fusion gene and upstream TP (Figure 13).

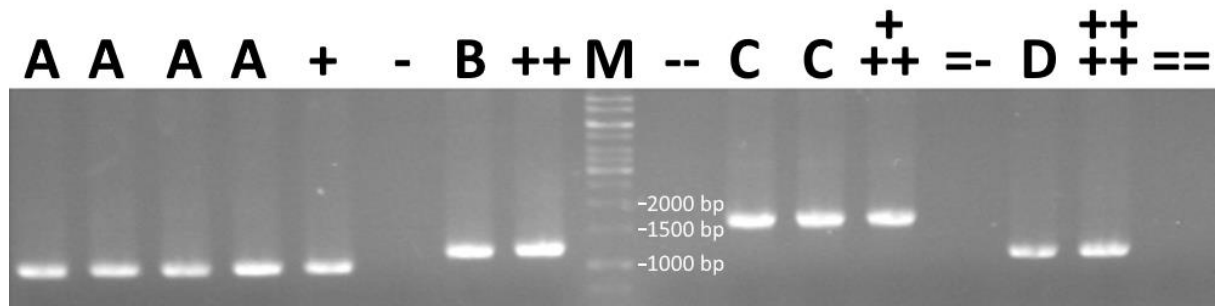


Figure 12 - Electrophoresis agarose gel of colony PCR screening of MS-ACC yEGFP fusion protein expression constructs. These PCRs verify the presence of gene and upstream TP. **A** (1036 bp), colony PCR screening for the pYPK0_TEF1_CAC1-yEGFP_TDH3 construct. +, positive control for A by using pYPK0_TEF1_CAC1_TDH3 as template. -, negative control for A by use of no template. **B** (1216 bp), colony PCR screening for the pYPK0_TDH3_CAC2-yEGFP_PGI1 construct. ++, positive control for B by using pYPK0_TDH3_CAC2_PGI1 as template. --, negative control for B by use of no template. **C** (1626 bp), colony PCR screening for the pYPK0_PGI1_CAC3-yEGFP_FBA1 construct. +++, positive control for C by using pYPK0_PGI1_CAC3_FBA1 as template. =-, negative control for C by use of no template. **D** (1087 bp), colony PCR screening for the pYPK0_FBA1_accDin-yEGFP_PDC1 construct. +++++, positive control for D by using pYPK0_FBA1_accDi_PDC1 as template. ==, negative control for D by use of no template. **M**, molecular weight marker.

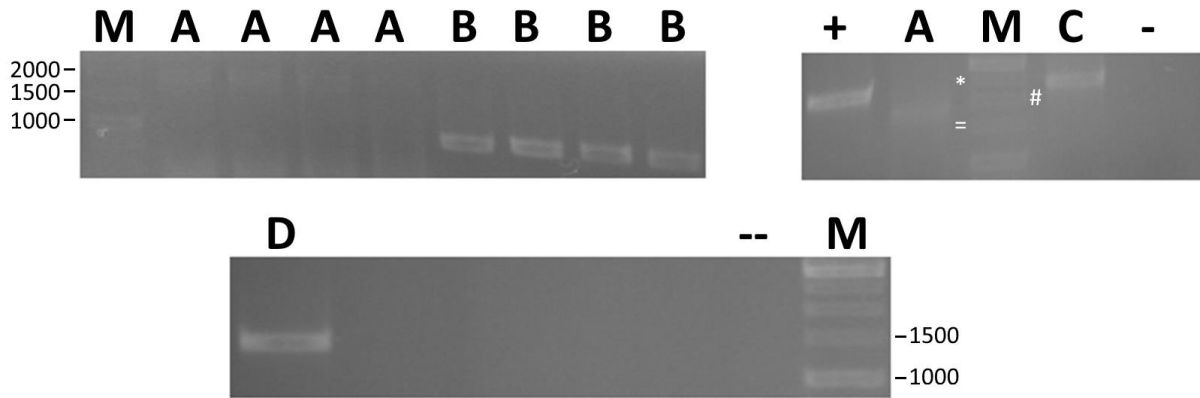


Figure 13 – Electrophoresis agarose gel of MS-ACC genes PCR amplification with addition of a linker coding sequence. Wells with no symbol or band are failed attempts at amplification. **A** (1727 bp), *CAC2linker* amplification at a T_A of 45 °C for the first 10 cycles, and 67 °C for the remaining 25 cycles (primers 1058 and 1051) . **B** (899 bp), *CAC1linker* amplification at a T_A of 50 °C for the first 10 cycles, and 68 °C for the remaining 25 cycles (primers 968 and 1052) . **A** (2366 bp), *CAC3linker* amplification at a T_A of 47 °C for the first 10 cycles, and 68 °C for the remaining 25 cycles (primers 972 and 1050). **D** (1526 bp), *accDinlinker* amplification at a T_A of 50 °C for the first 10 cycles, and 70 °C for the remaining 25 cycles (primers). **+** (2366 bp), positive control for *CAC3* amplification by using pYPK0_PGI1_ *CAC3*_FBA1 as template. **-**, negative control for *CAC3* amplification by use of no template. **--**,negative control for *accDin* amplification by use of no template. **M**, molecular weight marker. Relevant molecular weight marker bands: * (2500 bp); # (2000 bp); = (1500 bp).

Clones containing the various γ EGFP fusion constructs were visualized by fluorescence microscopy (Figure 14).

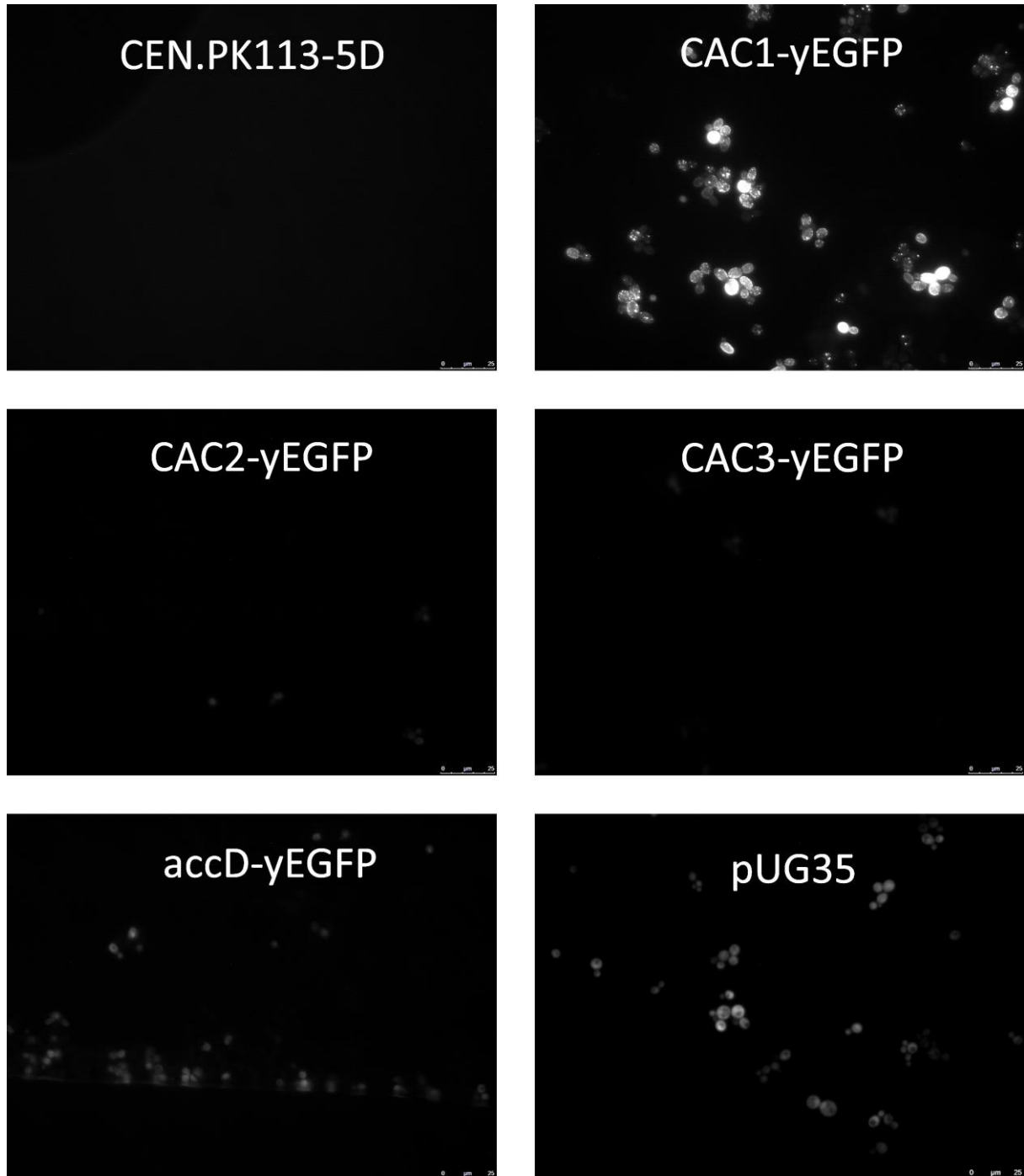


Figure 14 – Fluorescence microscopy images of different constructs. **CAC1- γ EGFP**, clone containing the pYPK0_TEF1_CAC1- γ EGFP_TDH3 construct. **CAC2- γ EGFP**, clone where pYPK0_TDH3_CAC2- γ EGFP_PGI1 was assembled. **CAC3- γ EGFP**, clone containing the pYPK0_PGI1_CAC3- γ EGFP_FBA1 construct. **accD- γ EGFP**, clone containing the pYPK0_FBA1_accDin- γ EGFP_PDC1 construct. **CEN.PK113-5D**, wild-type CENP.PK113-5D cells. **pUG35**, clone containing the pUG35 plasmid.

Sequencing confirmed the correct assembly of all but one of the constructs: pYPK0_TDH3_CAC2-yEGFP_PGI1 lacked the downstream TP (PGI1), which is probably the reason behind the lack of fluorescence displayed by the clone containing this construct. This, however, does not explain why pYPK0_PGI1_CAC3-yEGFP_FBA1 did not display fluorescence. Transcription of this gene was regulated by an established constitutive promoter present in PGI1 (Pereira et al., 2016) which makes failure in transcription an unlikely reason for this result. Clones containing the pYPK0_FBA1_accDin-yEGFP_PDC1 construct seem to display some cytosolic fluorescence in a somewhat similar fashion to clones containing pUG35. This is the expected result. Since *accD* does not possess a signal peptide sequence, the CT- β protein is expected to accumulate in the cytosol. Clones containing the pYPK0_FBA1_accDin-yEGFP_PDC1 construct displayed an interesting result. The BCCP1 protein seemed to be accumulating in specific cellular organelles. It is also possible that this accumulation is due to aggregation of misfolded proteins (Vieira Gomes et al., 2018).

3.2.3 Expression of genes without target peptide

In plants, signal peptides are usually cleaved upon arrival in the plastid, and thereafter not needed for protein function (Armbruster et al., 2009). The GFP expression results seem to insinuate that the signal peptides might be related to the absence of ACC activity in the clones containing the MS-ACC constructs. In order to circumvent this, the pYPK0_CAC1-ps_CAC2-ps_CAC3-ps_accDin construct was created. The MS-ACC genes without signal peptides used in this construct were amplified from cDNA of *A. thaliana* (Figure 15)

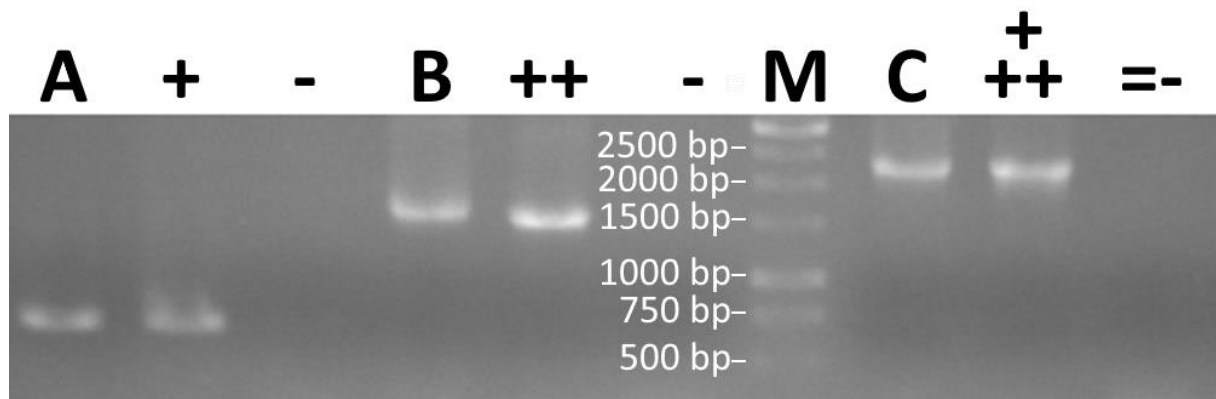


Figure 15 – Electrophoresis agarose gel of MS-ACC amplifications without signal peptides. **A** (600 bp), amplification of *CAC1-ps*. +, positive control for A by using pYPK0_TEF1_ *CAC1*_TDH3 as template. -, negative control for A by use of no template (primers 1047 and 967). **B** (1461 bp), amplification of *CAC2-ps*. ++, positive control for B by using pYPK0_TDH3_ *CAC2*_PGI1 as template. --, negative control for B by use of no template (primers 1046 and 969). **C** (2151 bp), amplification of *CAC3-ps*. +++, positive control for C by using pYPK0_PGI1_ *CAC3*_FBA1 as template. ==, negative control for C by use of no template (primers 1045 and 971).

Screening for correctly assembled constructs was performed by amplifying the genes and upstream TPs (Figure 16). Without signal peptides, *CAC1-ps* does not contain the sequence to which the primer used for the TEF1_ *CAC1* confirmation (primer 1067) would attach. Since *CAC1-ps* is a small sequence (600 bp), it was possible to screen for the pYPK0_TEF1_ *CAC1-ps*_TDH3 construct by amplifying the entire gene and downstream TP by use of primers 577 and 467. All cassettes used for the assembly of the pYPK0_ *CAC1-ps*_ *CAC2-ps*_ *CAC3-ps*_ *accDin* construct were confirmed via sequencing. Δ Acc Tet containing the pYPK0_ *CAC1-ps*_ *CAC2-ps*_ *CAC3-ps*_ *accDin* construct failed to grow on solid YPD Tet (Figure 20).

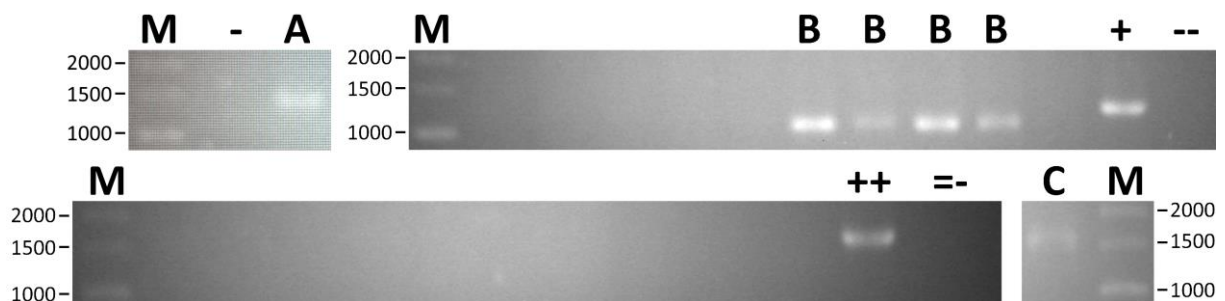


Figure 16 – Electrophoresis agarose gel of colony PCR screening of MS-ACC constructs without signal peptide. These PCRs verify the presence of gene and upstream TP. **A** (1450 bp), colony PCR screening for the pYPK0_TEF1_ *CAC1-ps*_TDH3 construct. -, negative control for A by use of no template. **B** (1009 bp), colony PCR screening for the pYPK0_TDH3_ *CAC2-ps*_PGI1 construct. + (1216 bp), positive control for B by using pYPK0_TDH3_ *CAC2*_PGI1 as template. --, negative control for B by use of no template. **C** (1467 bp), colony PCR screening for the pYPK0_PGI1_ *CAC3-ps*_FBA1 construct. ++ (1626 bp), positive control for C by using pYPK0_PGI1_ *CAC3*_FBA1 as template. ==, negative control for C by use of no template. **M**, molecular weight marker (values in bp).

3.2.4 Expression with activated accD

A. thaliana *accD* gene is posttranscriptionally regulated by a RNA editing that changes the cytosine in the position 794 to uracil. This converts the original Ser codon to Leu and is needed for the β -CT subunit to function (Salie & Thelen, 2016). Sequencing of the *accD* sequence used in the assembly of constructs pYPK0_CAC1_CAC2_CAC3_accDin and pYPK0_CAC1-ps_CAC2-ps_CAC3-ps_accDin show that this version accD version is the inactive form of the CDS (Figure 17). This is a possible reason for why none of these constructs were able to complement the conditional ACC1 null mutation found in Δ Acc Tet.

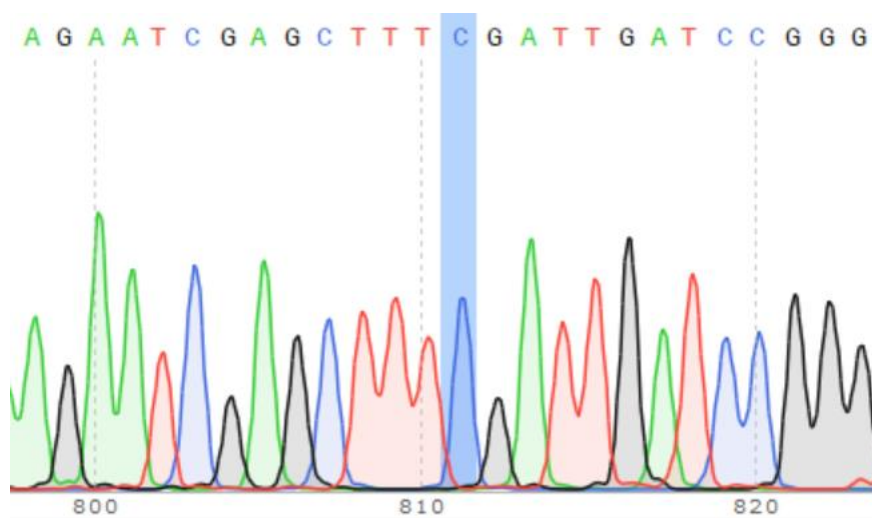


Figure 17 – SnapGene® software (from GSL Biotech; available at snapgene.com) DNA chromatogram of sequenced *accDin* displaying the presence of a cytosine in the position 794. The cytosine in question is highlighted in blue.

accDac was created via homologous recombination of fragments *accDF* and *accDT*. These fragments were successfully amplified by primers that substitute the cytosine in the 794 position by a thymine (Figure 18). This *accDac* was used to create the pYPK0_FBA1_ *accDac*_PDC1 construct which was screened by colony PCR (Figure 19).

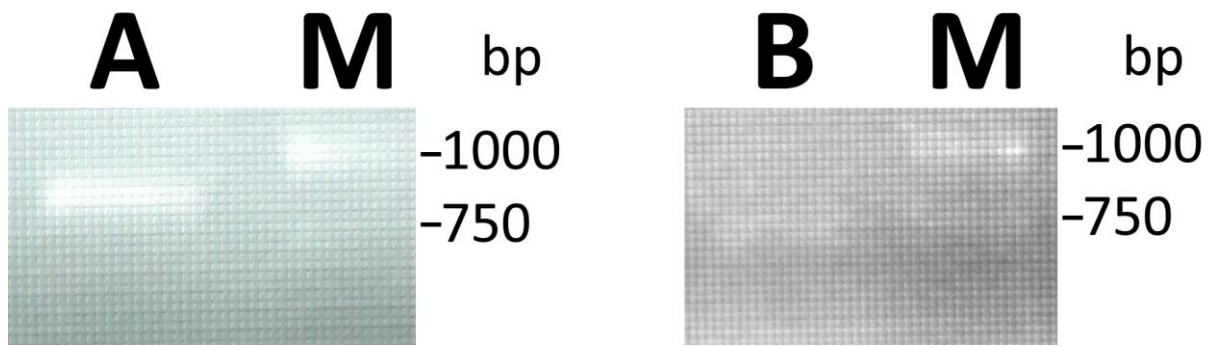


Figure 18 – Electrophoresis agarose gel of fragments accDF and accDT amplification at a T_A of 59 °C. **A** (847 bp), accDF amplification (primers 1057 and accD_C->T_rv). **B** (721 bp), accDT amplification (primers accD_C->T_fw and 973). **M**, molecular weight marker.

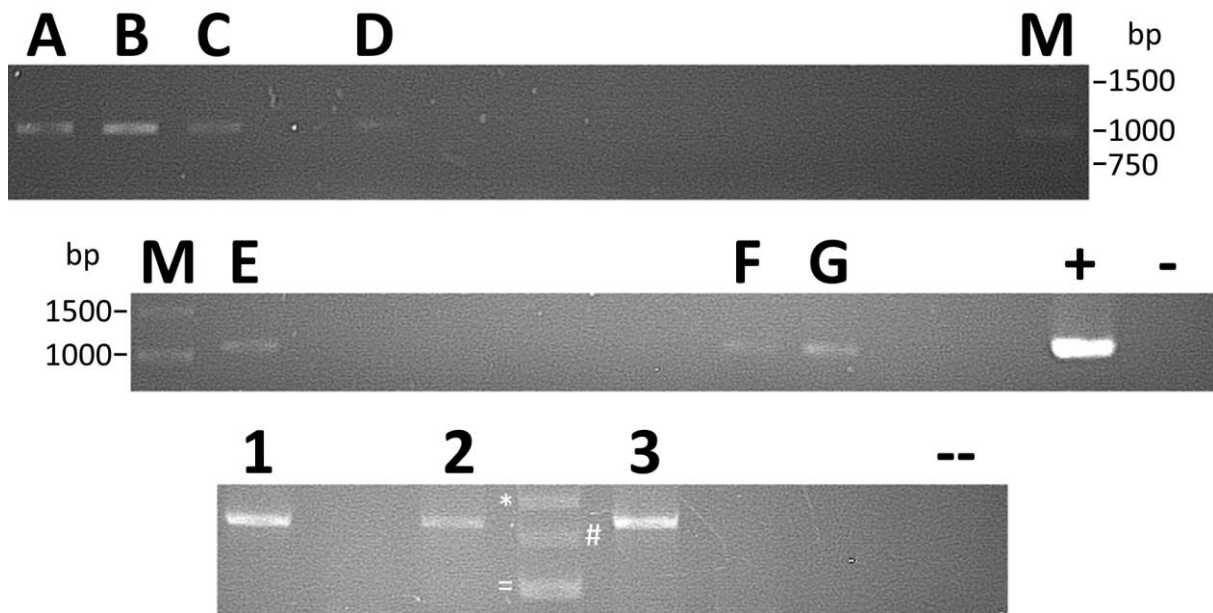


Figure 19 – Electrophoresis agarose gel of colony PCR screening of pYPK0_FBA1_accDac_PDC1. Letters are colony PCRs using primers 577 and 1064 (1090 bp). Numbers are colony PCRs using primers 1060 and 578 (1694 bp). **A** and **1**, **C** and **2**, and **D** and **3** are successful screenings of the same colonies. **B**, **E**, **F** and **G** are colonies that could only be verified for the presence of accDac and FBA1. **+**, positive control for the letter conditions using a previously extracted pYPK0_FBA1_accDin_PDC1 as template. **-**, negative control for letter conditions by use of no template. **--**, negative control for number conditions by use of no template **M**, molecular weight marker. . Relevant molecular weight marker bands: * (2000 bp); # (1500 bp); = (1000 bp).

The following MS-ACC multiple gene cluster expression constructs containing the active form of *accD* were assembled in Δ Acc Tet: TEF1_CAC1_TDH3_CAC2_PGI1_CAC3_FBA1_accDac_PDC1; TEF1_CAC1-ps_TDH3_CAC2-ps_PGI1_CAC3-ps_FBA1_accDac_PDC1; TEF1_CAC1-ps_TDH3_CAC2_PGI1_CAC3-ps_FBA1_accDac_PDC1; TEF1_CAC1-ps_TDH3_CAC2-ps_PGI1_Cac3_FBA1_accDac_PDC1; TEF1_CAC1_TDH3_CAC2_RPL5_Cac3_FBA1_accDin_PDC1. None of these constructs was capable of complementing the conditional *ACC1* null mutation of Δ Acc Tet (Figure 20). TEF1_CAC1-ps_TDH3_CAC2-ps_PGI1_CAC3-ps_FBA1_accDac_PDC1 and TEF1_CAC1-ps_TDH3_CAC2_PGI1_CAC3-ps_FBA1_accDac_PDC1 were confirmed via colony PCR (Figure 21)

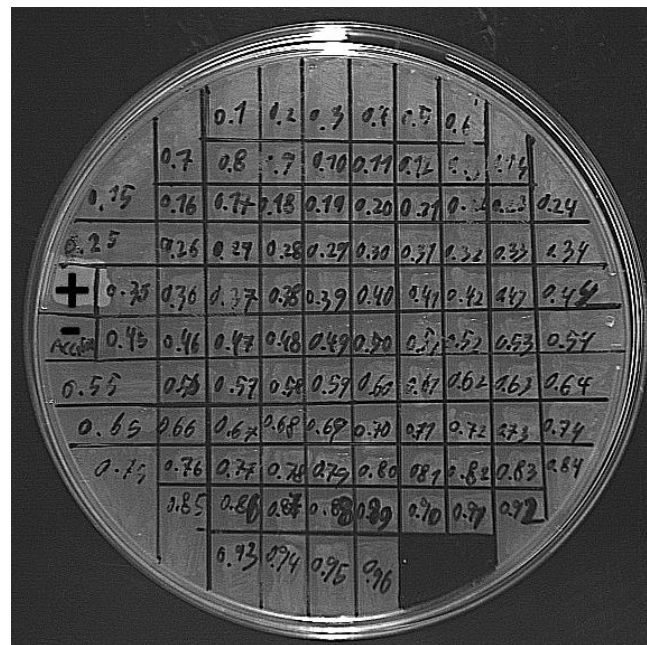


Figure 20 – Δ Acc Tet colonies containing a MS-ACC multiple gene cluster expression construct are unable to grow on solid YPD Tet medium. +, CEN.PK2-1C was used as positive control. -, Δ Acc Tet with no plasmid was used as negative control. Each of other marked divisions contains a single clone where TEF1_CAC1_TDH3_CAC2_PGI1_CAC3_FBA1_accDac_PDC1 was assembled. These results are representative of all the MS-ACC multiple gene cluster expression constructs that failed to complement conditional *ACC1* null mutation of Δ Acc Tet.

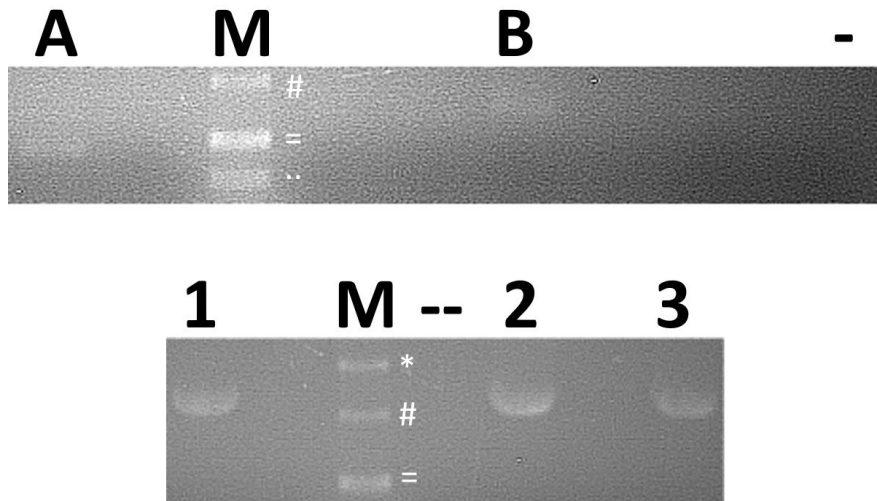


Figure 21 - Electrophoresis agarose gel of colony PCR screening of TEF1_CAC1-ps_TDH3_CAC2-ps_PGI1_CAC3-ps_FBA1_accDac_PDC1 and TEF1_CAC1-ps_TDH3_CAC2_PGI1_CAC3-ps_FBA1_accDac_PDC1. Letters are colony PCRs using primers 1063 and 1066 (972 bp for the construct containing CAC2-ps and 1179 for the other). Numbers are colony PCRs using primers 1061 and 1064 (1715 bp). **A** and **1**, and **B** and **3** are successful screenings of the same clones. **2**, clone that could only be verified for the presence of *CAC3* and *accDac*. -, negative control for letter conditions by use of no template. --, negative control for number conditions by use of no template. **M**, molecular weight marker. Relevant molecular weight marker bands: * (2000 bp); # (1500 bp); = (1000 bp); ..(750 bp).

3.2.5 *CAC2* gene and failure to complement conditional *ACC1* null mutation

The sequencing of *CAC2* showed that sequence of this fragment did not completely match with the theoretical sequence. A 76 bp sequence was found at position 1564 (Figure 22). Searching this sequence using the NCBI BLAST pointed to it being a *CAC2* intron. This is strange, given that the fragment was obtained from cDNA and no other *CAC2* introns were found within the sequenced fragment. The presence of this intron leads to a frame shift in the amplified gene which is a likely reason for why MS-ACC failed to display ACC activity when expressed in Δ Acc Tet. One function of RNA splicing is the posttranscriptional regulation of gene expression (Chorev & Carmel, 2012). In plants, some intron-retaining transcripts are stored and only spliced to allow protein expression when the required conditions arise (Boothby et al., 2013; Fankhauser & Aubry, 2017). It is possible that this was the reason for why an intron was present in *CAC2* amplified from cDNA.

```

      *           *           *           *           *           *           *           *
1499 ttgaggatttcaaaaatggaaaagttgatacagctttcatcgtcaagcatgaagaggagctagctgag----- 1566
      |           |           |           |           |           |           |           |
      |           |           |           |           |           |           |           |
922  TTGAGGATTTCAAAAATGGAAAAGTTGATACAGCTTTCATCGTCAAGCATGAAGAGGAGCTAGCTGAGGTAAATTCGAGTGTCTCTGTGGTGGGCTAAAG 1021
      *           *           *           *           *           *           *           *
      *           *           *           *           *           *           *           *
1567 -----tgggatatgaagcctttggtaaaagctgaacatagagataggagaattgcatgagaa 1622
      |           |           |           |           |           |           |           |
1022 ACACAGGCCATTGGATGTATTCATTTCAATGCTTCTAAGTTAGTGGGATATGAAGCCTTTGGTAAAGCTGAACATAGAGATAGGAGAATTGCATGAGAA 1121
      *           *           *           *           *           *           *           *

```

Figure 22 – ApE mediated comparison between theoretical *CAC2* (upper sequence) and amplified *CAC2* (bottom sequence).

One of the main problems with trying to express a multi-subunit enzyme is the difficulty in determining what subunits are the culprits for the absence of enzymatic activity. Without a simple way of screening for the proper performance of each individual subunit, this is a challenging prospect. Furthermore, the correct expression of the various subunits might not be the only problem. Differences between the ideal environmental conditions for protein function and the environment present in the expression host can also result in defective enzymatic activity. Plastidic ACC is mainly active during photosynthesis and various changes to the plastidic internal environment during this process have been shown to activate this enzyme. One of the most important of these is the change in pH from 7.1 to 8 (Salie & Thelen, 2016). The cytosol of yeast is maintained at a pH of 7.2 which might be not suitable for the function of plastidic ACC (Martínez-Muñoz & Kane, 2008; Orij et al., 2009; Y Sasaki et al., 1997).

3.3 Functional expression of *Y. lipolytica ACC1* in *S. cerevisiae*

Y. lipolytica is an oleaginous yeast capable of achieving a lipid content of 40% of dry weight (Beopoulos et al., 2009). Native overexpression of *ACC1* in this yeast has been previously successfully used to increase lipid content by 2 fold (Tai & Stephanopoulos, 2013). Similarly to *S. cerevisiae*, the ACC of this yeast is a multifunctional protein and is encoded by *YIACC1*. This gene could not be amplified by using tailed primers. However, amplification was successful when one of the primers was a tailed primer and the other was not. By using this strategy, fragments *YIACC1α* (primers 781 and 505) and *YIACC1β* (primers 504 and 782) were successfully amplified (Figure 23). The two fragments were then used both in the same transformation solution so that *YIACC1α* conferred homology to *TEF1* and *YIACC1β* conferred homology to *TDH3*. ΔAcc Tet cells overexpressing *YIACC1* were able to grow on solid YPD Tet (Figure 24). The presence of the correctly assembled construct was verified by colony PCR (Figure 25).

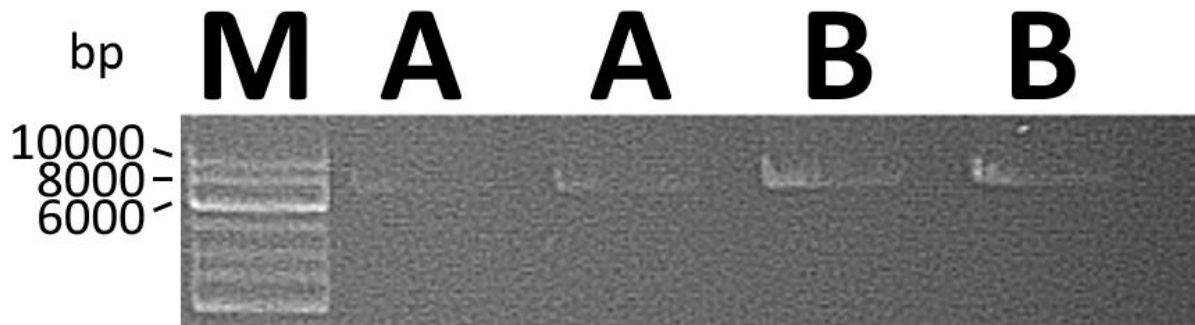


Figure 23 – Electrophoresis agarose gel of Phusion polymerase PCR amplification of both *YACC1* fragments at T_A of 60°C. **A** (7312 bp), amplification of *YACC1 α* fragment **B** (7304 bp), amplification of *YACC1 β* fragment. **M**, molecular weight marker.

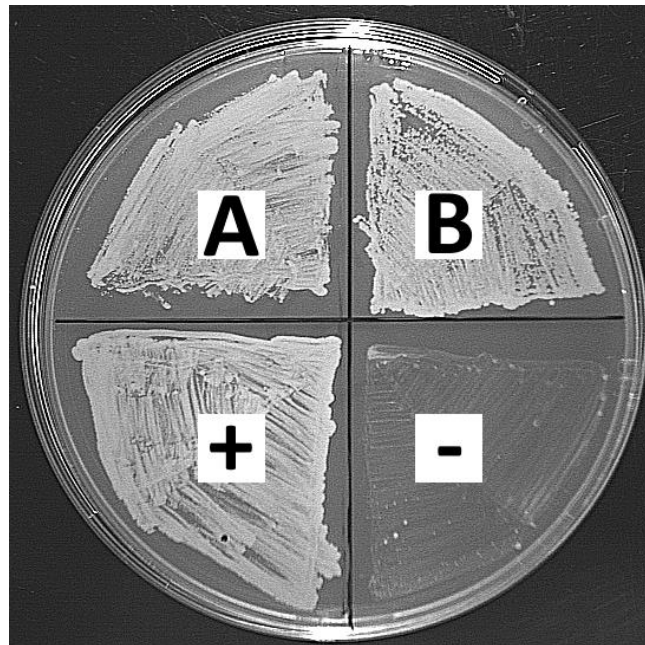


Figure 24 - Complementation of a conditional *ACC1* null mutation by pYPK0_TEF1_ScACC1_TDH3 on solid YPD Tet medium. **A**, Δ Acc Tet containing pYPK0_TEF1_ScACC1_TDH3. **+**, CEN.PK2-1C was used as positive control. **-**, Empty Δ Acc Tet is used as negative control. **M**, molecular weight marker.

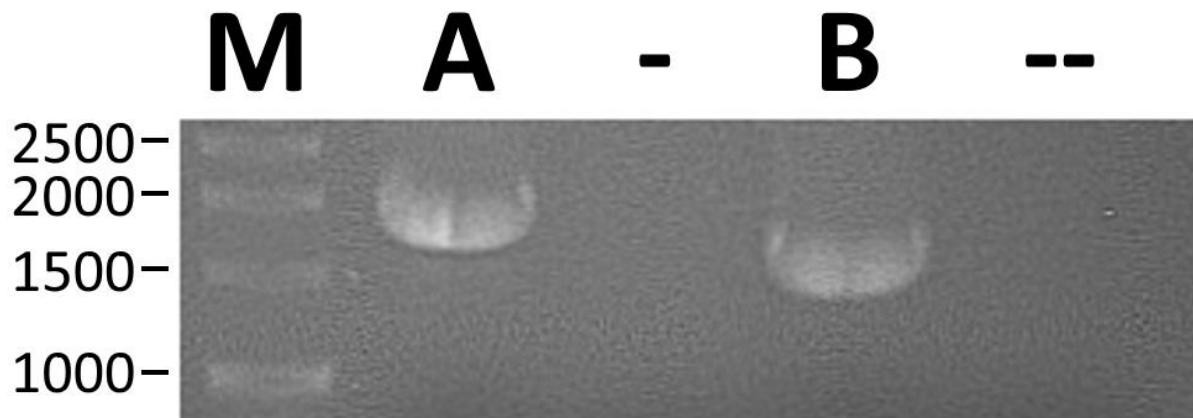


Figure 25 - Electrophoresis agarose gel of colony PCR screening of pYPK0_TEF1_YIACC1_TDH3 construct. A (1935 bp), PCR of pYPK0_TEF_YIACC1_TDH3 using primers 577 and 564. -, negative control of A by use of no template. B (1573 bp), PCR of pYPK0_TEF_YIACC1_TDH3 using primers 586 and 578. --, negative control of B by use of no template.

3.3.1 Specific growth rate of clones expressin ScACC1 or YIACC1

The Δ Acc Tet cells containing the constructs that displayed ACC activity when grown on solid YPD Tet medium were chosen for further testing. Growth curves were plotted for a wild type CEN.PK2-1C clone, a Δ Acc Tet clone without a plasmid, a Δ Acc Tet clone transformed with pYPKpw, a Δ Acc Tet clone overexpressing *ScACC1* and a Δ Acc Tet clone overexpressing *YIACC1* in liquid YPD Tet medium. Apart from *ScACC1* overexpressing and CEN.PK2-1C clones, every clone displayed a small initial growth that stopped at an OD of 0.2-0.9 (Figures 26 and 27). This growth was probably sustained by intracellular reserves of malonyl-CoA and likely stopped when those were exhausted (Joachimiak et al., 1997). *YIACC1* overexpressing cells took longer to reach exponential phase of growth than *ScACC1* overexpressing cells which, in turn, took longer than wild type CEN.PK2-1C cells (Figure 27). This difference might be a possible indication of a period of adaptation while the cells are switching from relying on the native ACC1 to relying on the recombinant variant.

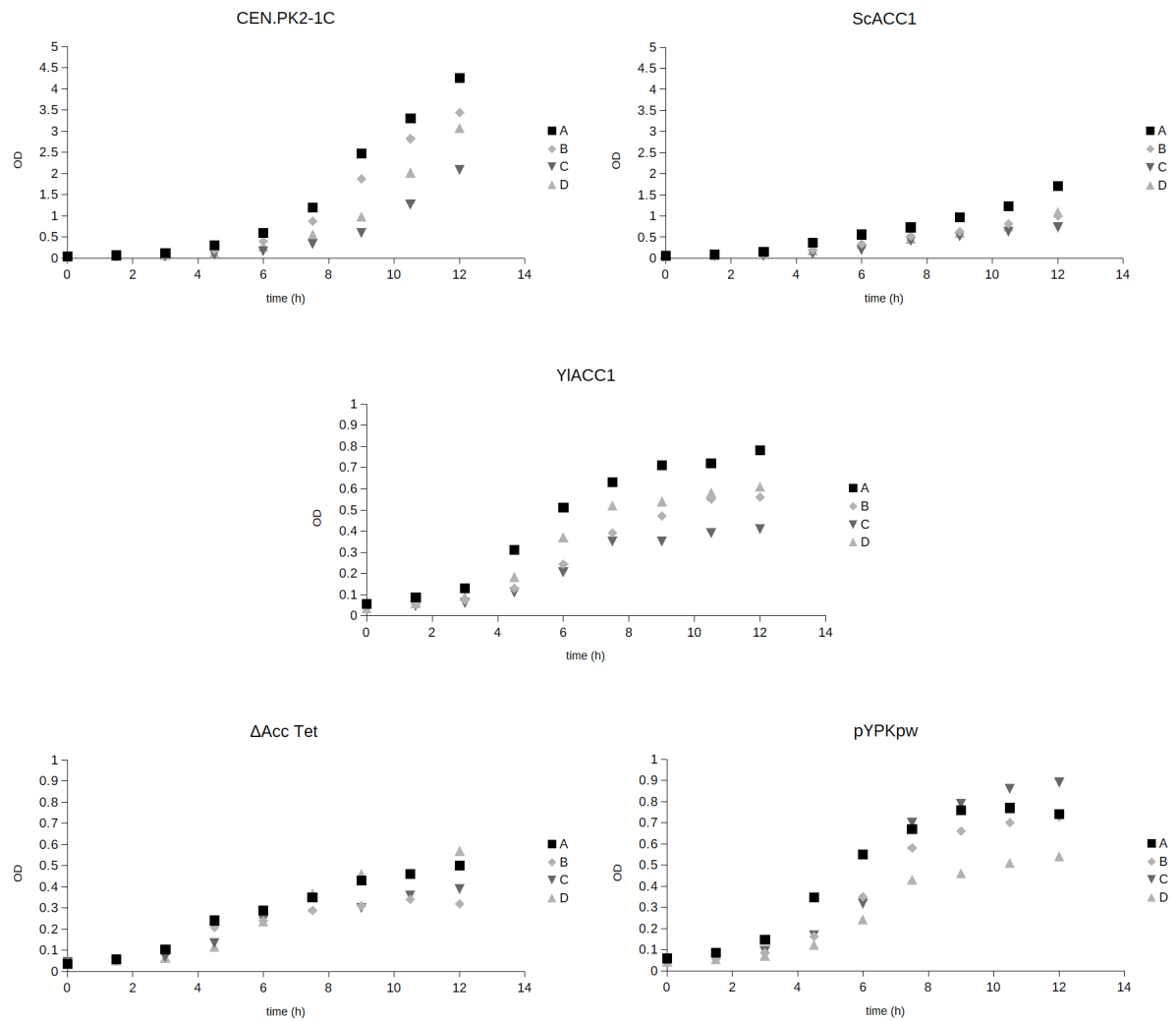


Figure 26 – Growth curves displaying the first 12h of growth in liquid YPD Tet. Each graphic plots the OD₆₄₀ over time(h) for one of the 5 colonies measured: **CEN.PK2-1C**, wild type CEN.PK2-1C clone; **Δ Acc Tet**, Δ Acc Tet clone without a plasmid; **pYPKpw**, Δ Acc Tet clone transformed with pYPKpw; **ScACC1**, Δ Acc Tet clone overexpressing *ScACC1*; **YIACC1**, Δ Acc Tet clone overexpressing *YIACC1*. The different letters represent different repeats of the same inoculums. Inoculums of different colonies that were measured simultaneously are represented by the same letter in the different graphics. All axes are expressed in a linear scale.

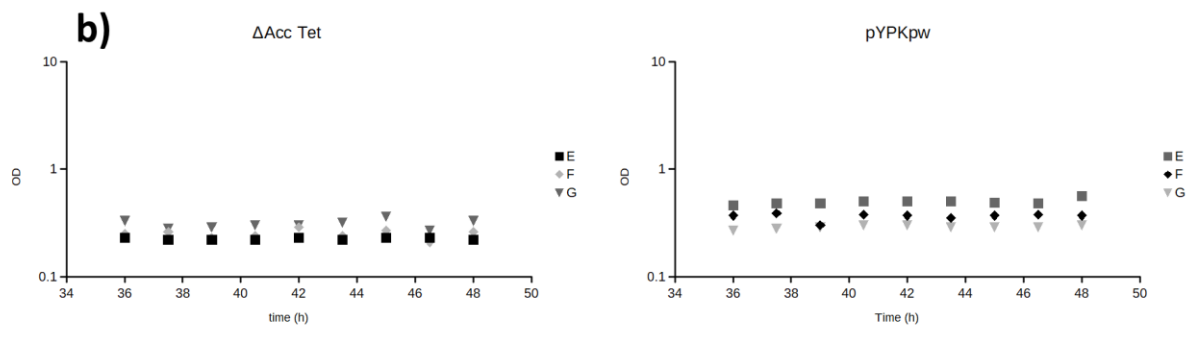
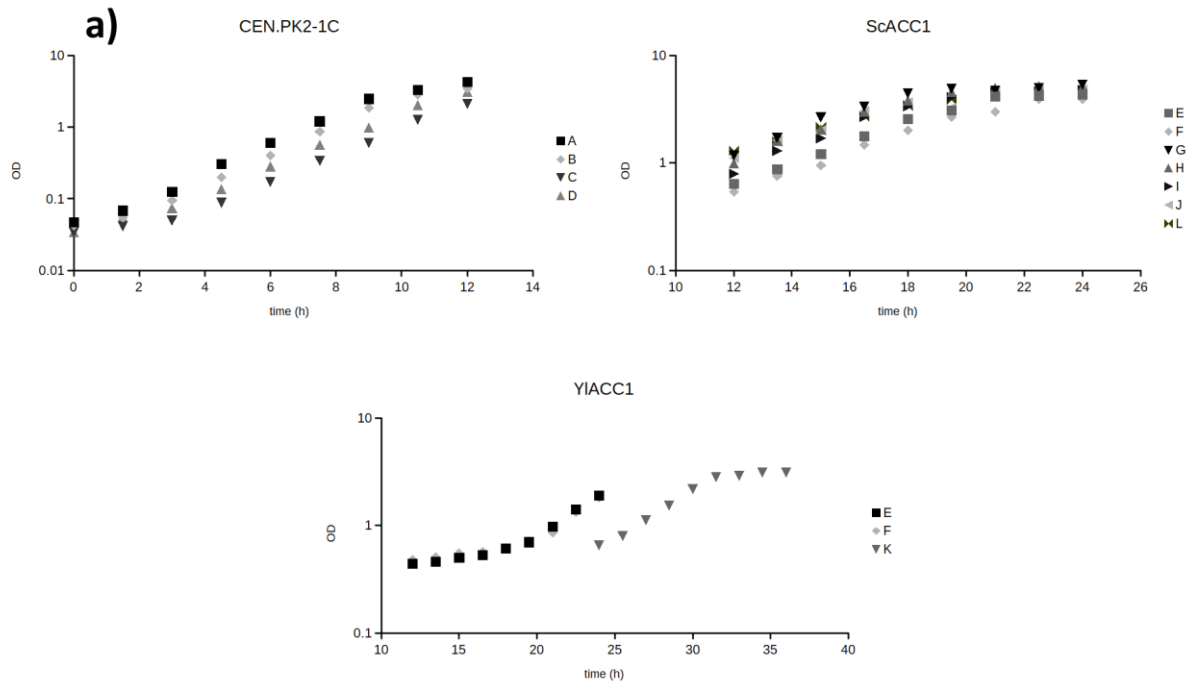


Figure 27 – a) Growth curves displaying the 12h or 24h (in the case of YIACC1) spans of time where the exponential growth phase was present for the strains that were capable of continuing growth in YPD Tet after the first 12h. **b)** Growth curves displaying the last 12h span of time for the strains that did not display additional growth after the first 12h. Each graphic plots the OD_{640} over time(h) for one of the 5 colonies measured: **CEN.PK2-1C**, wild type CEN.PK2-1C clone; **Δ Acc Tet**, Δ Acc Tet clone without a plasmid; **pYPKpw**, Δ Acc Tet clone transformed with pYPKpw; **ScACC1**, Δ Acc Tet clone overexpressing *ScACC1*; **YIACC1**, Δ Acc Tet clone overexpressing *YIACC1*. The different letters represent different repeats of the same inoculums. Inoculums of different clones that were measured simultaneously are represented by the same letter in the different graphics. The X axis is expressed in a linear scale. The Y axis is expressed in a logarithmic scale in order to allow for visualization of the exponential growth phase.

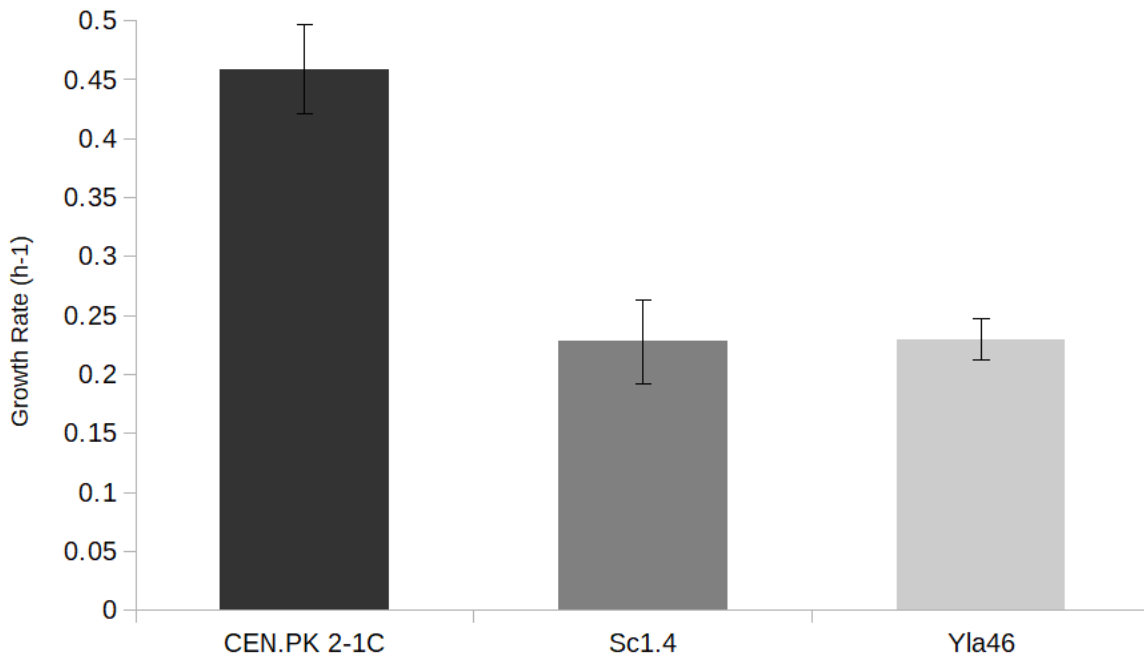


Figure 28 – Comparison between growth rates (h^{-1}) of wild-type CEN.PK2-1C and $\Delta\text{Acc Tet}$ containing either pYPK0_TEF1_*ScACC1*_TDH3 construct (ScACC1) or pYPK0_TEF1_*YIACC1*_TDH3 construct (YIACC1).

Overexpression of either of the *ACC1* genes resulted in a reduced specific growth rate (0.23 h^{-1} for *ScACC1* and *YIACC1*) when compared to the wild-type CEN.PK2-1C (0.47 h^{-1}) (Figure 28). This reduction in growth is consistent with previous studies where ACC activity was increased. Shi et al., 2014 compared overexpression of *S. cerevisiae* wild-type *ACC1*, *ACC1*^{S1157A} and *ACC1*^{S659AS1157A} and discovered that the *ACC1* variants that displayed greater ACC activity also possessed a reduced growth rate. This seems to indicate that this reduction in growth is not due to accumulation of the protein itself, but due to ACC activity. If this is the case, this reduction in growth can be caused by an imbalanced metabolism which can lead to either the depletion of essential intermediates or the accumulation of intermediates to toxic levels. A study in bacteria also supports this hypothesis. D. Liu et al., 2015 overexpressed both *S. cerevisiae* *ACC1* and the native MS-ACC genes in *E.coli*. Both ACCs increased fatty acid production and both proved to be toxic. Furthermore, when the authors used a malonyl-CoA sensor to control ACC expression based on intracellular malonyl-CoA concentration, the toxic effects of ACC overexpression were reduced and the fatty acid productivity was increased by 34%.

3.4 MCR production

MCR is an enzyme capable of reducing malonyl-CoA in two steps, generating malonic semialdehyde which is then converted 3-hydroxypropionate. This process simultaneously oxidizes 2 nicotinamide adenine dinucleotide phosphate (NADPH) molecules which can be detected spectrophotometrically through diminution of absorbance at 365 nm. By coupling the production of malonyl-coA by ACC to this reaction, ACC activity can be quantified by measuring NADPH oxidation (Kroeger et al., 2011). MCR was successfully extracted from *E. coli* BL21(DE3) containing pTrc-McrCa (Figure 29). By using this tool the ACC activity could be measured *in vitro*. However the monetary costs associated with this endeavor, prevented the continuation of this approach.

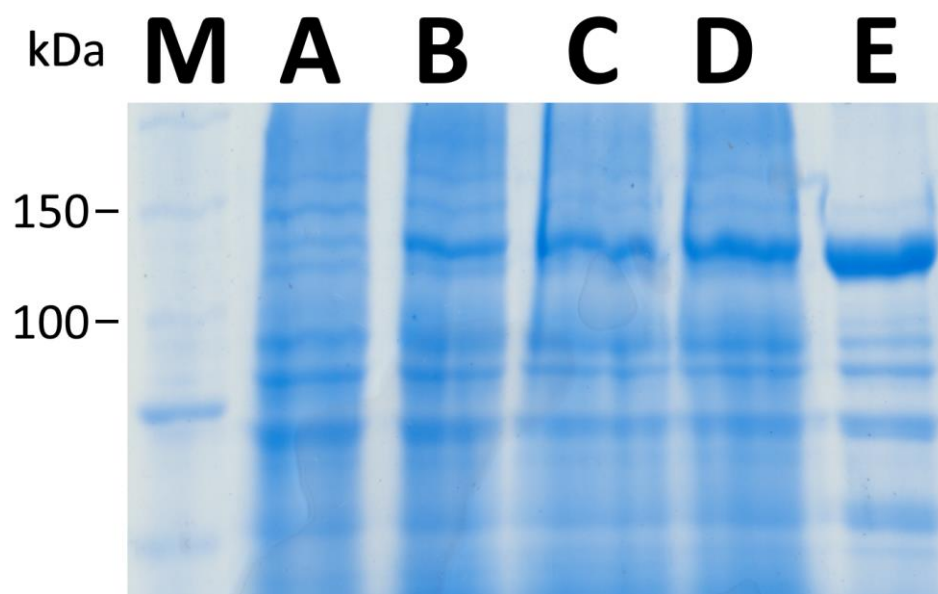


Figure 29 - SDS-PAGE polyacrymide gel of MCR protein (132 kDa). **A**, BL21(DE3) containing pTrc-McrCa at time of IPTG induction. **B**, BL21(DE3) containing pTrc-McrCa 2h after IPTG induction. **C**, BL21(DE3) containing pTrc-McrCa 4h after IPTG induction. **D**, BL21(DE3) containing pTrc-McrCa 6h after IPTG induction. **E**, MCR protein purified 4h after IPTG induction. **M**, molecular weight marker.

4. CONCLUSION AND FUTURE PERSPECTIVES

S. cerevisiae is a microorganism with a multitude of industrial applications, which include production of biopharmaceuticals and biofuel. However, the range of compounds that this yeast can produce in economically viable amounts is limited to those not derived malonyl-CoA. The reason for this is the small malonyl-CoA pool that this yeast possesses. The present work tries to solve this problem by heterologous expression of two ACCs from species capable of accumulating malonyl-CoA derived products in great amounts (*A. thaliana* and *Y. lipolytica*).

The Δ Acc Tet strain was capable of assessing whether an ACC gene carried by a plasmid was being functionally expressed. This strain was capable of growing on solid YPD Tet when transformed with a plasmid carrying a *S. cerevisiae* ACC1 expression cassette.

The heterologous expression of MS-ACC from *A. thaliana* in *S. cerevisiae* was unsuccessful at complementing the phenotype of Δ Acc Tet in tetracycline. Various hypotheses for this failure are presented and tackled in this work: the targeting of MS-ACC subunits to intracellular compartments other than the cytosol; the use of the inactive form of the *accD* gene that was amplified from cDNA. The addressing of these setbacks, however, was not enough to functionally express MS-ACC in *S. cerevisiae*. Other hypotheses remained untested, chief among them: the presence of an intron in the CAC2 sequence amplified from *A. thaliana* cDNA inactivates the respective protein; the potential inadequacy of *S. cerevisiae* cytosol to provide suitable conditions for MS-ACC activation. In future work, the first untested hypothesis could be addressed by the expression of a multiple gene cluster expression construct containing a CAC2 version without the intron. This version of the gene could be obtained by PCR amplification from cDNA of tissues with high CAC2 expression levels.

Functional expression of *ACC1* from *Y. lipolytica* in *S. cerevisiae* was capable of complementing the conditional *ACC1* null mutation of Δ Acc Tet. Even though the level of ACC activity was not quantified, the overexpression of both *ScACC1* and *YIACC1* resulted in reduced growth rate, which is linked to increased ACC activity in *S. cerevisiae*. The testing of this hypothesis could be done by *in vitro* enzymatic assays where ACC activity can be measured by coupling the malonyl-CoA generating reaction to the production of a fluorescent product (Choi & Da Silva, 2014) or to the consumption of a spectrophotometrically measurable reagent (Kroeger et al., 2011). The latter method was the one intended to be used in this work. MCR was successfully extracted from *E. coli* BL21(DE3) expressing

this protein. However, enzymatic assays had to be cancelled due to economic constraints. Cheaper methods do exist, however. The utilization of biosensors that express green fluorescent protein (GFP) at levels dependent on intracellular concentration of malonyl-CoA has been previously reported in *S. cerevisiae* (Xiaoxu Chen et al., 2018; David et al., 2016). These sensors are based in the FapR transcription factor and respective operator (*fapO*) of *Bacillus subtilis* that control the expression of genes related to lipid metabolism. The binding of malonyl-CoA to FapR inactivates this repressor and allows the regulated genes to be expressed (Schujman et al., 2006). By expressing FapR and inserting *fapO* near the transcription start site of a GFP expression cassette a malonyl-CoA sensor can be created. GFP fluorescence can then be measured *in vivo* by either fluorescence spectroscopy (Xiaoxu Chen et al., 2018) or flow cytometry (David et al., 2016).

In future work, the overexpression of ACCs from other oleaginous yeasts in *S. cerevisiae* could be an interesting prospect. Similarly to ScAcc1p, YIAcc1p is negatively regulated by Snf1p. In fact, in *Y. lipolytica* *Snf1* deletion led to an increase in fatty acid accumulation of 2.6 fold (Seip et al., 2013). It would be, therefore, desirable to use an *ACC1* whose protein is not regulated by Snf1p mediated phosphorylation. The Snf1p and AMPK are highly conserved in eukaryotes (M. Zhang et al., 2013). The target motif for serine phosphorylation of Snf1p/AMPK is a hydrophobic residue (M,L,F,I or V) for P-5 and P + 4, and basic residues (R,K or H) for P-3 or P-4 (Choi & Da Silva, 2014). By doing a protein BLAST (Johnson et al., 2008) for ScAcc1p, homologous proteins can be uncovered. It would then be possible to search these proteins for sequences not containing the serine phosphorylation target motif of Snf1p/AMPK. Heterologous expression of the respective genes could then be used to discover if these proteins are capable of enhancing ACC activity in *S. cerevisiae*.

5. BIBLIOGRAPHY

- Adams, I. P., Dack, S., Dickinson, F. M., & Ratledge, C. (2002). The distinctiveness of ATP:citrate lyase from *Aspergillus nidulans*. *Biochimica et Biophysica Acta - Protein Structure and Molecular Enzymology*, 1597(1), 36–41.
- Al-Qahtani, A., Teilhet, M., & Mensa-Wilmot, K. (1998). Species-specificity in endoplasmic reticulum signal peptide utilization revealed by proteins from *Trypanosoma brucei* and *Leishmania*. *The Biochemical Journal*, 331(Pt 2), 521–529.
- Araya-Cloutier, C., den Besten, H. M. W., Aisyah, S., Gruppen, H., & Vincken, J. P. (2017). The position of prenylation of isoflavonoids and stilbenoids from legumes (Fabaceae) modulates the antimicrobial activity against Gram positive pathogens. *Food Chemistry*, 226, 193–201.
- Armbruster, U., Hertle, A., Makarenko, E., Zühlke, J., Pribil, M., Dietzmann, A., ... Leister, D. (2009). Chloroplast proteins without cleavable transit peptides: Rare exceptions or a major constituent of the chloroplast proteome? *Molecular Plant*, 2(6), 1325–1335.
- Atabani, A. E., Silitonga, A. S., Badruddin, I. A., Mahlia, T. M. I., Masjuki, H. H., & Mekhilef, S. (2012). A comprehensive review on biodiesel as an alternative energy resource and its characteristics. *Renewable and Sustainable Energy Reviews*, 16(4), 2070–2093.
- Azevedo, F., Pereira, H., & Johansson, B. (2017). Colony PCR. In *PCR - Methods and Protocols* (Vol. 1620, pp. 129–139).
- Bachmair, A., & Varshavsky, A. (1989). The degradation signal in a short-lived protein. *Cell*, 56(6), 1019–1032.
- Baeshen, N. A., Baeshen, M. N., Sheikh, A., Bora, R. S., Ahmed, M. M. M., Ramadan, H. A. I., ... Redwan, E. M. (2014). Cell factories for insulin production. *Microbial Cell Factories*, 13(1), 0–9.
- Barnett, J. A. (2003). Beginnings of microbiology and biochemistry: The contribution of yeast research. *Microbiology*, 149(3), 557–567.
- Batra, P., & Sharma, A. K. (2013). Anti-cancer potential of flavonoids: recent trends and future perspectives. *3 Biotech*, 3(6), 439–459.
- Beckner, M., Ivey, M. L., & Phister, T. G. (2011). Microbial contamination of fuel ethanol fermentations. *Letters in Applied Microbiology*, 53(4), 387–394.
- Benson, D. A., Karsch-Mizrachi, I., Lipman, D. J., Ostell, J., & Wheeler, D. L. (2005). GenBank. *Nucleic Acids Research*, 33(DATABASE ISS.), 34–38.

- Beopoulos, A., Cescut, J., Haddouche, R., Uribebarrea, J. L., Molina-Jouve, C., & Nicaud, J. M. (2009). *Yarrowia lipolytica* as a model for bio-oil production. *Progress in Lipid Research*, 48(6), 375–387.
- Böer, E., Steinborn, G., Kunze, G., & Gellissen, G. (2007). Yeast expression platforms. *Applied Microbiology and Biotechnology*, 77(3), 513–523.
- Boothby, T. C., Zipper, R. S., Van der Weele, C. M., & Wolniak, S. M. (2013). Removal of Retained Introns Regulates Translation in the Rapidly Developing Gametophyte of *Marsilea vestita*. *Developmental Cell*, 24(5), 517–529.
- Borodina, I., & Nielsen, J. (2014). Advances in metabolic engineering of yeast *Saccharomyces cerevisiae* for production of chemicals. *Biotechnology Journal*, 9(5), 609–620.
- Chen, H., Kim, H. U., Weng, H., & Browse, J. (2011). Malonyl-CoA Synthetase, Encoded by *ACYL ACTIVATING ENZYME13*, Is Essential for Growth and Development of *Arabidopsis*. *The Plant Cell*, 23(6), 2247–2262.
- Chen, W. N., & Tan, K. Y. (2013). Malonate uptake and metabolism in *Saccharomyces cerevisiae*. *Applied Biochemistry and Biotechnology*, 171, 44–62.
- Chen, X., Yang, X., Shen, Y., Hou, J., & Bao, X. (2017). Increasing Malonyl-CoA Derived Product through Controlling the Transcription Regulators of Phospholipid Synthesis in *Saccharomyces cerevisiae*. *ACS Synthetic Biology*, 6(5), 905–912.
- Chen, X., Yang, X., Shen, Y., Hou, J., & Bao, X. (2018). Screening phosphorylation site mutations in yeast acetyl-CoA carboxylase using malonyl-CoA sensor to improve malonyl-CoA-derived product. *Frontiers in Microbiology*, 9(JAN), 1–8.
- Chen, X., Zaro, J. L., & Shen, W. C. (2013). Fusion protein linkers: Property, design and functionality. *Advanced Drug Delivery Reviews*, 65(10), 1357–1369.
- Chen, Y., Bao, J., Kim, I. K., Siewers, V., & Nielsen, J. (2014). Coupled incremental precursor and co-factor supply improves 3-hydroxypropionic acid production in *Saccharomyces cerevisiae*. *Metabolic Engineering*, 22, 104–109.
- Chen, Y., & Nielsen, J. (2013). Advances in metabolic pathway and strain engineering paving the way for sustainable production of chemical building blocks. *Current Opinion in Biotechnology*, 24(6), 965–972.
- Cherubini, F. (2010). The biorefinery concept: Using biomass instead of oil for producing energy and chemicals. *Energy Conversion and Management*, 51(7), 1412–1421.
- Choi, J. W., & Da Silva, N. a. (2014). Improving polyketide and fatty acid synthesis by engineering of the yeast acetyl-CoA carboxylase. *Journal of Biotechnology*, 187, 56–59.

- Choo, K. H., Tan, T. W., & Ranganathan, S. (2009). A comprehensive assessment of N-terminal signal peptides prediction methods. *BMC Bioinformatics*, *10*(SUPPL. 15), 1–12.
- Chorev, M., & Carmel, L. (2012). The function of introns. *Frontiers in Genetics*, *3*(55), 1–15.
- Costa, C. E., Romani, A., Cunha, J. T., Johansson, B., & Domingues, L. (2017). Integrated approach for selecting efficient *Saccharomyces cerevisiae* for industrial lignocellulosic fermentations: Importance of yeast chassis linked to process conditions. *Bioresource Technology*, *227*, 24–34.
- Crawford, J. M., & Townsend, C. A. (2010). New insights into the formation of fungal aromatic polyketides. *Nature Reviews Microbiology*, *8*(12), 879–889.
- Cronan, J. E., & Waldrop, G. L. (2002). Multi-subunit acetyl-CoA carboxylases. *Progress in Lipid Research*, *41*, 407–435.
- David, F., Nielsen, J., & Siewers, V. (2016). Flux Control at the Malonyl-CoA Node through Hierarchical Dynamic Pathway Regulation in *Saccharomyces cerevisiae*. *ACS Synthetic Biology*, *5*(3), 224–233.
- Davis, M. W. (2016). ApE - A plasmid Editor. <http://biologylabs.utah.edu/jorgensen/wayned/ape/>.
- Fakas, S. (2017). Lipid biosynthesis in yeasts: A comparison of the lipid biosynthetic pathway between the model nonoleaginous yeast *Saccharomyces cerevisiae* and the model oleaginous yeast *Yarrowia lipolytica*. *Engineering in Life Sciences*, *17*(3), 292–302.
- Fankhauser, N., & Aubry, S. (2017). Post-transcriptional regulation of photosynthetic genes is a key driver of C4leaf ontogeny. *Journal of Experimental Botany*, *68*(2), 137–146.
- Feng, X., Lian, J., & Zhao, H. (2015). Metabolic engineering of *Saccharomyces cerevisiae* to improve 1-hexadecanol production. *Metabolic Engineering*, *27*, 10–19.
- Galdieri, L., Zhang, T., Rogerson, D., Lleshi, R., & Vancura, A. (2014). Protein acetylation and acetyl coenzyme a metabolism in Budding Yeast. *Eukaryotic Cell*, *13*(12), 1472–1483.
- Gashaw, A., Getachew, T., & Teshita, A. (2015). A Review on Biodiesel Production as Alternative Fuel. *Journal of Forest Products & Industries*, *4*(2), 80–85. Retrieved from <http://researchpub.org/journal/jfpi/number/vol4-no2/vol4-no2-7.pdf>
- Gibson, D. G. (2009). Synthesis of DNA fragments in yeast by one-step assembly of overlapping oligonucleotides. *Nucleic Acids Research*, *37*(20), 6984–6990.
- Gietz, R. D., & Schiestl, R. H. (2008). High-efficiency yeast transformation using the LiAc / SS carrier DNA / PEG method. *Nature Protocols*, *2*(1), 31–35.
- Goffeau, A., Barrell, B. G., Bussey, H., Davis, R. W., Dujon, B., Feldmann, H., ... Oliver, S. G. (1996). Life with 6000 Genes conveniently among the different interna- Old Questions and New Answers

- The genome . At the beginning of the se- of its more complex relatives in the eukary- cerevisiae has been completely sequenced Schizosaccharomyces pombe indicate. *Science*, 274(October), 546–567.
- González, R., Ballester, I., López-Posadas, R., Suárez, M. D., Zarzuelo, A., Martínez-Augustin, O., & Sánchez de Medina, F. (2011). Effects of flavonoids and other polyphenols on inflammation. *Critical Reviews in Food Science and Nutrition*, 51(4), 331–362.
- Haar, T. v d, Jossé, L. J., & Byrne, L. J. (2007). 8 Reporter Genes and Their Uses in Studying Yeast Gene Expression. *Methods in Microbiology*, 36(06), 165–188.
- Hasan, M. M., & Rahman, M. M. (2017). Performance and emission characteristics of biodiesel–diesel blend and environmental and economic impacts of biodiesel production: A review. *Renewable and Sustainable Energy Reviews*, 74(C), 938–948.
- Hofbauer, H. F., Schopf, F. H., Schleifer, H., Knittelfelder, O. L., Pieber, B., Rechberger, G. N., ... Kohlwein, S. D. (2014). Regulation of gene expression through a transcriptional repressor that senses acyl-chain length in membrane phospholipids. *Developmental Cell*, 29(6), 729–739.
- Hoja, U., Marthol, S., Hofmann, J., Stegner, S., Schulz, R., Meier, S., ... Schweizer, E. (2004). HFA1 encoding an organelle-specific acetyl-CoA carboxylase controls mitochondrial fatty acid synthesis in Saccharomyces cerevisiae. *Journal of Biological Chemistry*, 279(21), 21779–21786.
- Hu, X. H., Wang, M. H., Tan, T., Li, J. R., Yang, H., Leach, L., ... Luo, Z. W. (2007). Genetic dissection of ethanol tolerance in the budding yeast Saccharomyces cerevisiae. *Genetics*, 175(3), 1479–1487.
- Hunkeler, M., Stutfeld, E., Hagmann, A., Imseng, S., & Maier, T. (2016). The dynamic organization of fungal acetyl-CoA carboxylase. *Nature Communications*, 7.
- Ishtar Snoek, I. S., & Yde Steensma, H. (2007). Factors involved in anaerobic growth of Saccharomyces cerevisiae. *Yeast*.
- Joachimiak, M., Tevzadze, G., Podkowinski, J., Haselkorn, R., & Gornicki, P. (1997). Wheat cytosolic acetyl-CoA carboxylase complements an ACC1 null mutation in yeast. *Proceedings of the National Academy of Sciences of the United States of America*, 94(18), 9990–5.
- Johansson, B. (n.d.). WebPCR. Retrieved from <http://www.webpccr.appspot.com/>
- Johnson, M., Zaretskaya, I., Raytselis, Y., Merezhuk, Y., McGinnis, S., & Madden, T. L. (2008). NCBI BLAST: a better web interface. *Nucleic Acids Research*, 36(Web Server issue), 5–9.
- Jönsson, L. J., Alriksson, B., & Nilvebrant, N. O. (2013). Bioconversion of lignocellulose: Inhibitors and detoxification. *Biotechnology for Biofuels*, 6(1), 1–10.

- Kjeldsen, T. (2000). Yeast secretory expression of insulin precursors. *Applied Microbiology and Biotechnology*, *54*(3), 277–286.
- Klinner, U., & Schäfer, B. (2004). Genetic aspects of targeted insertion mutagenesis in yeasts. *FEMS Microbiology Reviews*, *28*(2), 201–223.
- Knoshaug, E. P., Van Wychen, S., Singh, A., & Zhang, M. (2018). Lipid accumulation from glucose and xylose in an engineered, naturally oleaginous strain of *Saccharomyces cerevisiae*. *Biofuel Research Journal*, *5*(2), 800–805.
- Koornneef, M., & Meinke, D. (2010). The development of *Arabidopsis* as a model plant. *Plant Journal*, *61*(6), 909–921.
- Korbie, D. J., & Mattick, J. S. (2008). Touchdown PCR for increased specificity and sensitivity in PCR amplification. *Nature Protocols*, *3*(9), 1452–1456.
- Kötter, P., Amore, R., Hollenberg, C. P., & Ciriacy, M. (1990). Isolation and characterization of the *Pichia stipitis* xylitol dehydrogenase gene, *XYL2*, and construction of a xylose-utilizing *Saccharomyces cerevisiae* transformant. *Current Genetics*, *18*(6), 493–500.
- Kötter, P., Weigand, J. E., Meyer, B., Entian, K.-D., & Suess, B. (2009). A fast and efficient translational control system for conditional expression of yeast genes. *Nucleic Acids Research*, *37*(18), e120.
- Kroeger, J. K., Zarzycki, J., & Fuchs, G. (2011). A spectrophotometric assay for measuring acetyl-coenzyme A carboxylase. *Analytical Biochemistry*, *411*(1), 100–105.
- Kumar, N., Varun, & Chauhan, S. R. (2013). Performance and emission characteristics of biodiesel from different origins: A review. *Renewable and Sustainable Energy Reviews*, *21*(C), 633–658.
- Li-Beisson, Y., Shorrosh, B., Beisson, F., Andersson, M. X., Arondel, V., Bates, P. D., ... Ohlrogge, J. (2013). Acyl-Lipid Metabolism. *The Arabidopsis Book*, *11*(e0161).
- Li, M., Schneider, K., Kristensen, M., Borodina, I., & Nielsen, J. (2016). Engineering yeast for high-level production of stilbenoid antioxidants. *Scientific Reports*, *6*, 1–8.
- Li, X., Guo, D., Cheng, Y., Zhu, F., Deng, Z., & Liu, T. (2014). Overproduction of fatty acids in engineered *Saccharomyces cerevisiae*. *Biotechnology and Bioengineering*, *111*(9), 1841–1852.
- Li, X., Ilarslan, H., Brachova, L., Qian, H.-R., Li, L., Che, P., ... Nikolau, B. J. (2011). Reverse-Genetic Analysis of the Two Biotin-Containing Subunit Genes of the Heteromeric Acetyl-Coenzyme A Carboxylase in *Arabidopsis* Indicates a Unidirectional Functional Redundancy. *Plant Physiology*, *155*(1), 293–314.
- Lian, J., & Zhao, H. (2014). Recent advances in biosynthesis of fatty acids derived products in *Saccharomyces cerevisiae* via enhanced supply of precursor metabolites. *Journal of Industrial*

- Microbiology and Biotechnology*, 42(3), 437–451.
- Liu, D., Xiao, Y., Evans, B., & Zhang, F. (2015). Negative feedback regulation of fatty acid production based on a malonyl-CoA sensor-actuator. *ACS Synthetic Biology*, 4(2), 132–140.
- Liu, W., Zhang, B., & Jiang, R. (2017). Improving acetyl-CoA biosynthesis in *Saccharomyces cerevisiae* via the overexpression of pantothenate kinase and PDH bypass. *Biotechnology for Biofuels*, 10(1), 1–9.
- Liu, X., Jia, B., Sun, X., Ai, J., Wang, L., Wang, C., ... Huang, W. (2015). Effect of Initial PH on Growth Characteristics and Fermentation Properties of *Saccharomyces cerevisiae*. *Journal of Food Science*, 80(4), M800–M808.
- Martinez-Muñoz, G. A., & Kane, P. (2008). Vacuolar and plasma membrane proton pumps collaborate to achieve cytosolic pH homeostasis in yeast. *Journal of Biological Chemistry*, 283, 20309–20319.
- McAleer, W. J., Buynak, E. B., Maigetter, R. Z., Wampler, D. E., Miller, W. J., & Hilleman, M. R. (1984). Human hepatitis B vaccine from recombinant yeast. *Nature*.
- Meng, X., Yang, J., Xu, X., Zhang, L., Nie, Q., & Xian, M. (2009). Biodiesel production from oleaginous microorganisms. *Renewable Energy*, 34(1), 1–5.
- Mirończuk, A. M., Rzechonek, D. A., Biegalska, A., Rakicka, M., & Dobrowolski, A. (2016). A novel strain of *Yarrowia lipolytica* as a platform for value-added product synthesis from glycerol. *Biotechnology for Biofuels*, 9(1), 1–12.
- Mohd Azhar, S. H., Abdulla, R., Jambo, S. A., Marbawi, H., Gansau, J. A., Mohd Faik, A. A., & Rodrigues, K. F. (2017). Yeasts in sustainable bioethanol production: A review. *Biochemistry and Biophysics Reports*, 10(March), 52–61.
- Moser, B. R. (2010). Camelina (*Camelina sativa* L.) oil as a biofuels feedstock: Golden opportunity or false hope? *Lipid Technology*, 22(12), 270–273.
- Mühlhausen, S., & Kollmar, M. (2014). Molecular phylogeny of sequenced *Saccharomycetes* reveals polyphyly of the alternative yeast codon usage. *Genome Biology and Evolution*, 6(12), 3222–3237.
- Nakagawa, S., Niimura, Y., Gojobori, T., Tanaka, H., & Miura, K. ichiro. (2008). Diversity of preferred nucleotide sequences around the translation initiation codon in eukaryote genomes. *Nucleic Acids Research*, 36(3), 861–871.
- Narendranath, N. V., & Power, R. (2005). Relationship between pH and medium dissolved solids in terms of growth and metabolism of lactobacilli and *Saccharomyces cerevisiae* during ethanol

- production. *Applied and Environmental Microbiology*, 71(5), 2239–2243.
- Novick, R. P. (1987). Plasmid incompatibility. *Microbiological Reviews*, 51(4), 381–395.
- O'Neill, C. M., Gill, S., Hobbs, D., Morgan, C., & Bancroft, I. (2003). Natural variation for seed oil composition in *Arabidopsis thaliana*. *Phytochemistry*, 64(6), 1077–1090.
- Orij, R., Postmus, J., Beek, A. Ter, Brul, S., & Smits, G. J. (2009). In vivo measurement of cytosolic and mitochondrial pH using a pH-sensitive GFP derivative in *Saccharomyces cerevisiae* reveals a relation between intracellular pH and growth. *Microbiology*, 155, 268–278.
- Paddon, C. J., Westfall, P. J., Pitera, D. J., Benjamin, K., Fisher, K., McPhee, D., ... Newman, J. D. (2013). High-level semi-synthetic production of the potent antimalarial artemisinin. *Nature*, 496(7446), 528–532.
- Papanikolaou, S., & Aggelis, G. (2011). Lipids of oleaginous yeasts. Part II: Technology and potential applications. *European Journal of Lipid Science and Technology*, 113(8), 1052–1073.
- Pereira, F., Azevedo, F., Parachin, N. S., Hahn-Hägerdal, B., Gorwa-Grauslund, M. F., & Johansson, B. (2016). Yeast Pathway Kit: A Method for Metabolic Pathway Assembly with Automatically Simulated Executable Documentation. *ACS Synthetic Biology*, 5(5), 386–394.
- Qiao, K., Imam Abidi, S. H., Liu, H., Zhang, H., Chakraborty, S., Watson, N., ... Stephanopoulos, G. (2015). Engineering lipid overproduction in the oleaginous yeast *Yarrowia lipolytica*. *Metabolic Engineering*, 29, 56–65.
- Ratledge, C. (2002). Regulation of lipid accumulation in oleaginous micro-organisms. *Biochemical Society Transactions*, 30(6), 1047–1050.
- Rodriguez, A., Strucko, T., Stahlhut, S. G., Kristensen, M., Svenssen, D. K., Forster, J., ... Borodina, I. (2017). Metabolic engineering of yeast for fermentative production of flavonoids. *Bioresource Technology*, 245, 1645–1654.
- Ruenwai, R., Cheevadhanarak, S., & Laoteng, K. (2009). Overexpression of Acetyl-CoA carboxylase gene of *Mucor rouxii* enhanced fatty acid content in *Hansenula polymorpha*. *Molecular Biotechnology*, 42(3), 327–332.
- Runguphan, W., & Keasling, J. D. (2014). Metabolic engineering of *Saccharomyces cerevisiae* for production of fatty acid-derived biofuels and chemicals. *Metabolic Engineering*, 21, 103–113.
- Salie, M. J., & Thelen, J. J. (2016). Regulation and structure of the heteromeric acetyl-CoA carboxylase. *Biochimica et Biophysica Acta - Molecular and Cell Biology of Lipids*, 1861(9), 1207–1213.
- Sandager, L., Gustavsson, M. H., Ståhl, U., Dahlqvist, A., Wiberg, E., Banas, A., ... Stymne, S. (2002). Storage lipid synthesis is non-essential in yeast. *Journal of Biological Chemistry*, 277(8), 6478–

6482.

- Sasaki, Y., Kozaki, a, & Hatano, M. (1997). Link between light and fatty acid synthesis: thioredoxin-linked reductive activation of plastidic acetyl-CoA carboxylase. *Proceedings of the National Academy of Sciences of the United States of America*, *94*(20), 11096–11101.
- Sasaki, Y., & Nagano, Y. (2004). Plant acetyl-CoA carboxylase: structure, biosynthesis, regulation, and gene manipulation for plant breeding. *Bioscience, Biotechnology, and Biochemistry*, *68*(6), 1175–1184.
- Schillera, J., Castellsagué, X., Villa, L., & Hildesheimd, A. (2008). An Update of Prophylactic Human Papillomavirus L1 Virus-Like Particle Vaccine Clinical Trial Results. *Vaccine*, *26*(Suppl 10), 1–18.
- Schujman, G. E., Guerin, M., Buschiazzo, A., Schaeffer, F., Llarrull, L. I., Reh, G., ... de Mendoza, D. (2006). Structural Basis of Lipid Biosynthesis Regulation in Gram-Positive Bacteria. *The EMBO Journal*, *25*(17), 4074–4083.
- Seip, J., Jackson, R., He, H., Zhu, Q., & Hong, S. P. (2013). Snf1 is a regulator of lipid accumulation in *Yarrowia lipolytica*. *Applied and Environmental Microbiology*, *79*(23), 7360–7370.
- Seleem, D., Pardi, V., & Murata, R. M. (2017). Review of flavonoids: A diverse group of natural compounds with anti-Candida albicans activity in vitro. *Archives of Oral Biology*, *76*, 76–83.
- Selvaraj, R., Praveenkumar, R., & Moorthy, I. G. (2016). A comprehensive review of biodiesel production methods from various feedstocks. *Biofuels*, *7*(269)(November), 1–9.
- Shao, Z., Zhao, H., & Zhao, H. (2009). DNA assembler, an in vivo genetic method for rapid construction of biochemical pathways. *Nucleic Acids Research*, *37*(2), 1–10.
- Sheff, M. A., & Thorn, K. S. (2004). Optimized cassettes for fluorescent protein tagging in *Saccharomyces cerevisiae*. *Yeast*, *21*(8), 661–670.
- Sheng, J., & Feng, X. (2015). Metabolic engineering of yeast to produce fatty acid-derived biofuels: Bottlenecks and solutions. *Frontiers in Microbiology*, *6*(JUN), 1–11.
- Shi, S., Chen, Y., Siewers, V., & Nielsen, J. (2014). Improving production of malonyl coenzyme A-derived metabolites by abolishing Snf1-dependent regulation of Acc1. *MBio*, *5*(3), 1–8.
- Shi, S., Valle-Rodríguez, J. O., Khoomrung, S., Siewers, V., & Nielsen, J. (2012). Functional expression and characterization of five wax ester synthases in *Saccharomyces cerevisiae* and their utility for biodiesel production. *Biotechnology for Biofuels*, *5*(1), 7.
- Shin, G. H., Veen, M., Stahl, U., & Lang, C. (2012). Overexpression of genes of the fatty acid biosynthetic pathway leads to accumulation of sterols in *saccharomyces cerevisiae*. *Yeast*, *29*(9), 371–383.

- Shin, S. Y., Jung, S. M., Kim, M. D., Han, N. S., & Seo, J. H. (2012). Production of resveratrol from tyrosine in metabolically engineered *Saccharomyces cerevisiae*. *Enzyme and Microbial Technology*, *51*(4), 211–216.
- Siewers, V. (2014). An Overview on Selection Marker Genes for Transformation of *Saccharomyces cerevisiae*. In V. Mapelli (Ed.), *Yeast Metabolic Engineering* (pp. 3–15). Hatfield, Hertfordshire, UK: Humana Press.
- Sun, Y., Sriramajayam, K., Luo, D., & Liao, D. J. (2012). A Quick, cost-free method of purification of DNA fragments from agarose gel. *Journal of Cancer*, *3*(1), 93–95.
- Tai, M., & Stephanopoulos, G. (2013). Engineering the push and pull of lipid biosynthesis in oleaginous yeast *Yarrowia lipolytica* for biofuel production. *Metabolic Engineering*, *15*(1), 1–9.
- Tehlivets, O., Scheuringer, K., & Kohlwein, S. D. (2007). Fatty acid synthesis and elongation in yeast. *Biochimica et Biophysica Acta - Molecular and Cell Biology of Lipids*, *1771*(3), 255–270.
- Thermofisher. (n.d.). Multiple Primer Analyzer. <https://www.thermofisher.com/pt/en/home/brands/thermo-scientific/molecular-biology/molecular-biology-learning-center/molecular-biology-resource-library/thermo-scientific-web-tools/multiple-primer-analyzer.html>.
- Tong, L., & Harwood, H. J. (2006). Acetyl-coenzyme A carboxylases: Versatile targets for drug discovery. *Journal of Cellular Biochemistry*, *99*(6), 1476–1488.
- Tsunematsu, Y., Ishiuchi, K., Hotta, K., & Watanabe, K. (2013). Yeast-based genome mining, production and mechanistic studies of the biosynthesis of fungal polyketide and peptide natural products. *Natural Product Reports*, *30*(8), 1139.
- Valle-Rodríguez, J. O., Shi, S., Siewers, V., & Nielsen, J. (2014). Metabolic engineering of *Saccharomyces cerevisiae* for production of fatty acid ethyl esters, an advanced biofuel, by eliminating non-essential fatty acid utilization pathways. *Applied Energy*, *115*, 226–232.
- Vieira Gomes, A., Souza Carmo, T., Silva Carvalho, L., Mendonça Bahia, F., & Parachin, N. (2018). Comparison of Yeasts as Hosts for Recombinant Protein Production. *Microorganisms*, *6*(2), 38.
- Wan, H., & Leclercq, A. (2012). *US008088623B2*. United States of America.
- Wan, H., Sjölander, M., Schairer, H. U., & Leclercq, A. (2004). A new dominant selection marker for transformation of *Pichia pastoris* to soraphen A resistance. *Journal of Microbiological Methods*, *57*(1), 33–39.
- Wang, G., Xiong, X., Ghogare, R., Wang, P., Meng, Y., & Chen, S. (2016). Exploring fatty alcohol-producing capability of *Yarrowia lipolytica*. *Biotechnology for Biofuels*, *9*(1), 1–10.

- Wang, J., Xu, R., Wang, R., Haque, M. E., & Liu, A. (2016). Overexpression of acc gene from oleaginous yeast lipomyces starkeyi enhanced the lipid accumulation in saccharomyces cerevisiae with increased levels of glycerol 3-Phosphate substrates. *Bioscience, Biotechnology and Biochemistry*, *80*(6), 1214–1222.
- Wang, Y., Chen, H., & Yu, O. (2014). A plant malonyl-CoA synthetase enhances lipid content and polyketide yield in yeast cells. *Applied Microbiology and Biotechnology*, *98*(12), 5435–5447.
- Wattanachaisaerekul, S., Lantz, A. E., Nielsen, M. L., Andrésson, Ó. S., & Nielsen, J. (2007). Optimization of heterologous production of the polyketide 6-MSA in Saccharomyces cerevisiae. *Biotechnology and Bioengineering*, *97*(4), 893–900.
- Wattanachaisaerekul, S., Lantz, A. E., Nielsen, M. L., & Nielsen, J. (2008). Production of the polyketide 6-MSA in yeast engineered for increased malonyl-CoA supply. *Metabolic Engineering*, *10*(5), 246–254.
- Wei, J., Zhang, Y., Yu, T. Y., Sadre-Bazzaz, K., Rudolph, M. J., Amodeo, G. A., ... Tong, L. (2016). A unified molecular mechanism for the regulation of acetyl-CoA carboxylase by phosphorylation. *Cell Discovery*, *2*, 1–12.
- Westfall, P. J., Pitera, D. J., Lenihan, J. R., Eng, D., Woolard, F. X., Regentin, R., ... Paddon, C. J. (2012). Production of amorphadiene in yeast, and its conversion to dihydroartemisinin acid, precursor to the antimalarial agent artemisinin. *Proceedings of the National Academy of Sciences*, *109*(3), E111–E118.
- Winzeler, E. A., Shoemaker, D. D., Astromoff, A., Liang, H., Anderson, K., Andre, B., ... Davis, R. W. (1999). Functional characterization of the S. cerevisiae genome by gene deletion and parallel analysis. *Science*, *285*(5429), 901–906.
- Wu, C. H., Apweiler, R., Bairoch, A., Natale, D. A., Barker, W. C., Boeckmann, B., ... Suzek, B. (2006). The Universal Protein Resource (UniProt): an expanding universe of protein information. *Nucleic Acids Research*, *34*(Database issue), D187-91.
- Yoshiyuki, H., Yasuki, F., Shigeyuki, K., Wataru, H., & Kousaku, M. (2002). Extremely simple, rapid, and highly efficient transformation method for the yeast Saccharomyces cerevisiae using glutathione and early log phase cells. *Journal of Bioscience and Bioengineering*, *94*(2), 166–171.
- You, S. K., Joo, Y.-C., Kang, D. H., Shin, S. K., Hyeon, J. E., Woo, H. M., ... Han, S. O. (2017). Enhancing Fatty Acid Production of Saccharomyces cerevisiae as an Animal Feed Supplement. *Journal of Agricultural and Food Chemistry*, *65*, 11029–11035.
- Zhang, M., Galdieri, L., & Vancura, A. (2013). The Yeast AMPK Homolog SNF1 Regulates Acetyl

Coenzyme A Homeostasis and Histone Acetylation. *Molecular and Cellular Biology*, 33(23), 4701–4717.

Zhang, S., Skerker, J. M., Rutter, C. D., Maurer, M. J., Arkin, A. P., & Rao, C. V. (2016). Engineering *Rhodospiridium toruloides* for increased lipid production. *Biotechnology and Bioengineering*, 113(5), 1056–1066.

Zheng, Y. N., Li, L. L., Liu, Q., Yang, J. M., Wang, X. W., Liu, W., ... Xian, M. (2012). Optimization of fatty alcohol biosynthesis pathway for selectively enhanced production of C12/14 and C16/18 fatty alcohols in engineered *Escherichia coli*. *Microbial Cell Factories*, 11(189), 1–11.

APPENDICES

Appendix I

Ramsdale amino acid mixture w/o Ura for SD URA- medium

Constituent	mg/L
L-adenine	19,74
L-arginine	78,96
L-asparagine	78,96
L-asparticacid	78,96
L-cysteine	78,96
L-glutamicacid	78,96
L-glutamine	78,96
L-glycine	78,96
L-isoleucine	78,96
L-lysine	78,96
L-methionine	78,96
L-phenylalanine	78,96
L-proline	78,96
L-serine	78,96
L-threonine	78,96
L-tyrosine	78,96
L-valine	78,96
myo-inositol	78,96
para-aminobenzidine	78,96
L-Histidine	80
L-Tryptophan	80
L-Leucine	400